

# **Optimal Orbit Transfers**

By

**Jeffrey Scott Parker**

February 2001  
Dr. Robert H. Tolson  
MAE 292

# Table of Contents

<b><u>INTRODUCTION</u></b> .....	1
LAWDEN'S PRIMER .....	2
<b><u>IMPULSIVE TRANSFERS</u></b> .....	6
COPLANAR TRANSFERS .....	6
<i>Single Impulse Transfers</i> .....	7
<i>Two-Impulse Transfers</i> .....	10
<i>Three-Impulse Transfers</i> .....	19
<i>N-Impulse Transfers</i> .....	27
NON-COPLANAR .....	29
<i>Hohmann Transfer with Split-Plane Change</i> .....	29
<i>Restricted Three-Impulse Plane Change</i> .....	32
<b><u>FINITE BURNS</u></b> .....	36
INDIRECT .....	36
DIRECT .....	39
<b><u>LOW THRUST</u></b> .....	45
<b><u>REFERENCES</u></b> .....	52

## List of Figures

Figure 1 Single impulse thrust junction point .....	8
Figure 2 Two-impulse transfer between identical ellipses .....	12
Figure 3 Characteristic velocity for orbit rotation .....	15
Figure 4 Hohmann transfer raising the orbit altitude .....	16
Figure 5 Possible eccentricities for transfer ellipse .....	18
Figure 6 Characteristic velocity for Hohmann and bi-elliptic transfers .....	20
Figure 7 Bi-elliptic transfer with exterior conjunction .....	21
Figure 8 Characteristic velocity for exterior conjunction bi-elliptic transfer .....	22
Figure 9 Derivative of characteristic velocity for exterior conjunction bi-elliptic transfer .....	23
Figure 10 Feasibility for $9 < r_3/r_1 < \rho_{crit}$ .....	25
Figure 11 Characteristic velocity for $1 \leq r_2/r_1 \leq r_3/r_1$ .....	26
Figure 12 Characteristic velocity for $r_2/r_1 < 1$ .....	26
Figure 13 Hohmann transfer with split plane change .....	30
Figure 14 Velocity vector triangles for Hohmann plane change impulses .....	30
Figure 15 Restricted three-impulse plane change .....	32
Figure 16 Restricted three-impulse plane change results .....	33
Figure 17 State and control variables .....	41
Figure 18 Two-burn finite thrust transfer trajectory .....	44
Figure 19 Three-burn finite thrust transfer trajectory .....	44
Figure 20 Steering angle versus time .....	49
Figure 21 Velocity versus time .....	50
Figure 22 Inclination versus time .....	50

## **Introduction**

Many satellites will require a change in the orbital elements during their lifetime. This change could be needed for a variety of reasons, such as transitioning to the final mission orbit after being launched into an initial parking orbit or correcting the orbital elements after perturbation effects have built up. Most often a change is made to orbit altitude or to the orbit plane or to both. To produce the change in orbital elements, a change must be made to the satellite velocity, either magnitude, direction, or both. Greater changes in velocity ( $\Delta V$ ) require greater amounts of propellant and hence have a higher cost. To reduce costs the amount of  $\Delta V$  needs to be reduced. Orbit transfers that minimize  $\Delta V$  are considered optimal.

This paper will present some of the current methods for optimal orbit transfers between co-planar and non-coplanar orbits of circular and elliptical shapes. The methods employ impulse, finite thrust, and low thrust transfers.

## Lawden's Primer

Letting  $Ox_1x_2x_3$  be three rectangular Cartesian coordinate axes forming an inertial reference frame. At some time  $t$  a spacecraft has position  $x_I (I=1, 2, 3)$  and velocity  $v_I$  relative to this frame. The equations of motion for this spacecraft can be written as

$$\dot{v} = \frac{cm}{M} l_i + g_i \quad (1)$$

$$\dot{x} = v \quad (2)$$

$$\dot{M} = -m \quad (3)$$

Here  $c$ , is the velocity of the exhaust particles,  $m$  is the rate of propellant use,  $M$  is the mass of the propellant within the spacecraft,  $l_I$  are the direction cosines of the direction of thrust, and  $g_I$  are components of gravitational acceleration. The  $l_I$  are constrained so that

$$l_1^2 + l_2^2 + l_3^2 = 1 \quad (4)$$

and  $m$  is constrained such that

$$m(\bar{m} - m) - a^2 = 0 \quad (5)$$

where  $\bar{m}$  is a maximum rate of propellant expenditure and  $a^2$  is a control variable with no physical significance and a value,  $a^2 \geq 0$ . When the control variables,  $l_I$ ,  $m$ , and  $a$  are known functions of  $t$ , then  $v_i$ ,  $x_i$ , and  $M$  can be determined with initial conditions

$$v_i = v_{i0}, x_i = x_{i0}, M = M_0 \quad (6)$$

at time  $t_0$ .

Employing the method of Lagrange multipliers produces the expression<sup>1</sup>

$$F = -\lambda_i \left( \frac{cm}{M} l_i + g_i \right) - \lambda_{i+3} v_i + \lambda_7 m + \mu_1 (l_1^2 + l_2^2 + l_3^2 - 1) + \mu_2 [m(\bar{m} - m) - a^2] \quad (7)$$

which leads to the equations for optimum conditions

$$\dot{\lambda}_i = -\lambda_{i+3} \quad (8)$$

$$\dot{\lambda}_{i+3} = -\lambda_j \frac{\partial g_j}{\partial x_i} \quad (9)$$

$$\dot{\lambda}_7 = \frac{cm}{M^2} \lambda_i l_i \quad (10)$$

$$0 = -\frac{cm}{M} \lambda_i + 2\mu_1 l_i \quad (11)$$

$$0 = -\frac{c}{M} \lambda_i l_i + \lambda_7 + \mu_2 (\bar{m} - 2m) \quad (12)$$

$$0 = -2\mu_2 a \quad (13)$$

The last equation requires that either  $\mu_2$ , or  $a$ , or both be equal to zero. When  $a = 0$ ,  $m = \bar{m}$  or zero. If  $\mu_2 = 0$ ,  $0 \leq m \leq \bar{m}$ . Therefore an optimal trajectory can have three different types of arcs within it, null thrust arcs where only gravity affects motion, maximum thrust arcs, and intermediate thrust arcs<sup>1</sup>.

Combining equations 8 and 9 produces

$$\dot{\lambda}_i = \lambda_j \frac{\partial g_j}{\partial x_i} \quad (14)$$

Since  $g_j$  are vector components,  $\frac{\partial g_j}{\partial x_i}$  acts as a second rank tensor. Therefore  $\lambda_i$  that satisfy equation 13 act as components of a vector. Lawden calls this vector the primer<sup>1</sup>. It will be denoted by  $\mathbf{p}$ . If  $m$  and  $\mu_1$  are both non-zero equation 11 requires that  $l_i$  be in the same ratio to each other as  $\lambda_i$ . This means that  $\mathbf{p}$  must be parallel to the thrust direction. If  $m=0$ , there is no thrust and  $l_i$  are indeterminate. If  $\mu_1=0$  the primer vanishes.

For an optimal trajectory, the Weierstrass condition<sup>1</sup> requires every point to satisfy

$$\left(\frac{c}{M}\lambda_i l_i - \lambda_7\right)m \geq \left(\frac{c}{M}\lambda_i l_i^* - \lambda_7\right)m^* \quad (15)$$

for all possible values of  $l_i^*$  and  $m^*$ , which are values of  $l_i$  and  $m$  that satisfy equations 4 and 5.

During a null thrust,  $m=0$  and equation 15 reduces to

$$\lambda_7 \geq \frac{c}{M}\lambda_i l_i^* \quad (16).$$

$\lambda_i l_i^*$  is the scalar product of the primer and the unit vector comprised of  $l_i^*$ . This product will be a maximum when the two vectors are aligned and will have a value equal to the magnitude,  $p = (\lambda_1^2 + \lambda_2^2 + \lambda_3^2)^{1/2}$ , of the primer. Equation 16 then becomes

$$\lambda_7 \geq \frac{c}{M}p \quad (17).$$

During a maximum thrust,  $m = \bar{m}$ , also setting  $m^* = \bar{m}$  reduces equation 15 to

$$\lambda_i l_i \geq \lambda_i l_i^* \quad (18).$$

Since  $m^* \leq \bar{m}$ , setting  $l_i^* = l_i$  in equation 15 requires that

$$\lambda_7 \leq \frac{c}{M}\lambda_i l_i \quad (19).$$

Equation 18 is satisfied for all  $l_i^*$  only if  $\lambda_i l_i$  is a maximum value for variations of  $l_i$ .

Since  $\lambda_i l_i$  is a scalar product of  $\lambda_i$  and  $l_i$ , the value will be a maximum when the two are aligned. Therefore, as shown earlier, the primer and the thrust must be in the same

direction. Equation 19 can then be written as

$$\lambda_7 \leq \frac{c}{M}p \quad (20).$$

For intermediate thrust,  $m^*$  can be greater than or less than  $m$ . When  $l_i^* = l_i$  in equation 15, the inequality is no longer valid for all  $m^*$ . Equality is still possible if

$$\lambda_7 = \frac{c}{M} \lambda_i l_i \quad (21).$$

Returning this value to equation 15 finds that

$$\lambda_7 \geq \frac{c}{M} \lambda_i l_i^* \quad (22)$$

for all  $l_i^*$ .  $\frac{c}{M} \lambda_i l_i^*$  will be a maximum when  $\lambda_i, l_i^*$  are aligned. As before this yields

$$\lambda_7 \geq \frac{c}{M} p \quad (23)$$

but equation 21 implies

$$\lambda_7 \leq \frac{c}{M} p \quad (24).$$

Therefore

$$\lambda_7 = \frac{c}{M} p \quad (25).$$

The results from the three cases above can be summarized as follows<sup>1</sup>:

- i) If thrust occurs and  $p \neq 0$ , the thrust must act in the direction of the primer.
- ii) If a function  $k$  is defined as

$$k = \frac{c}{M} p - \lambda_7 \quad (26).$$

then  $k \leq 0$  during null thrust,  $k \geq 0$  during maximum thrust, and  $k = 0$  during intermediate thrust.

## **Impulsive Transfers**

If it is assumed that the maximum thrust is not limited in magnitude and the duration of thrust is negligible compared to the orbit period, this thrust can be treated as an impulsive thrust. During an impulsive thrust, the spacecraft velocity is changed instantaneously while the position remains unchanged.

A point in an optimal trajectory where impulsive thrust is applied is referred to as a junction point. Across a junction point, position,  $x_i$ , is a continuous function of time. It follows, equation 14, that the primer and its first and second order derivatives are continuous.

Allowing impulsive thrusts, an optimal trajectory is a series of null thrusts connected at junction points. A trajectory of this type is subject to the following conditions<sup>1</sup>:

- a) The primer and its first time derivative must be continuous everywhere.
- b) At junction points, thrust must be aligned with the primer, which must have a certain constant magnitude  $P$ .
- c) During null thrust periods, the magnitude of the primer must not exceed  $P$ .

## **Coplanar Transfers**

Coplanar transfers occur when there is no change in orbital inclination between orbits. They are primarily used to raise or lower the orbit altitude. This is accomplished by respectively increasing or decreasing the orbital energy. Thrust vectors used to perform coplanar orbit transfers are in the orbit plane.

### *Single Impulse Transfers*

When the initial and final orbits contain at least one intersecting point, it is possible to perform the transfer through a single impulse at this point. If both sets of orbital elements are known, the impulse can be calculated and the primer can be determined at the junction point. The first two components of the primer in terms of orbital elements are given by Lawden as:

$$\lambda = A \cos f + B e \sin f \quad (27)$$

$$\mu = -A \sin f + B(1 + e \cos f) + \frac{D - A \sin f}{1 + e \cos f} \quad (28)$$

where  $f$  is the true anomaly,  $e$  the eccentricity, and  $A, B, D$  are constants. The third component is identically zero since all motion is confined to one plane. The derivative of these components are given as:

$$\xi = \frac{\gamma^{1/2}}{a^{3/2}} (A \sin f - B \cos f - D) \quad (29)$$

$$\eta = -\frac{\gamma^{1/2}}{a^{3/2}} (A \cos f - B \sin f) \quad (30)$$

Applying condition a) from the previous section,  $\dot{\mathbf{p}}$  is continuous at the junction point. Six conditions now exist to determine the values of  $A, B,$  and  $D$  at the junction point. The primer will then be defined by equations 27 and 28 everywhere. This transfer is then considered a relative optimum if the magnitude of this primer never exceeds unity. Consider the single impulse junction point shown in figure 1.

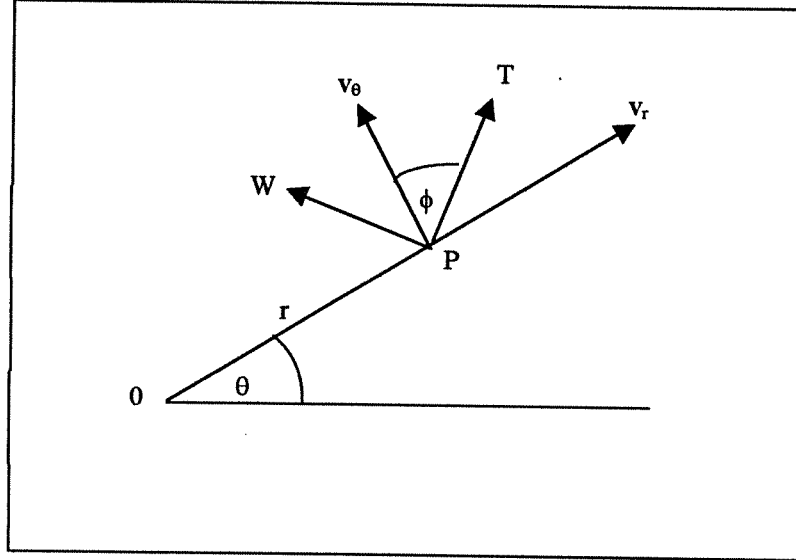


**Figure 1 Single impulse thrust junction point**

Here  $v_r$  and  $v_\theta$  are the radial and transverse components of the velocity at junction P in an orbit described by the semi-latus rectum,  $l$ , eccentricity,  $e$ , and argument of perigee,  $\omega$ . An impulsive thrust  $T$  is applied at an angle  $\phi$  from the perpendicular to the radius vector,  $r$ . A component of the spacecraft velocity, denoted by  $W$ , perpendicular to the direction of thrust will remain constant and can be expressed as

$$W = v_\theta \sin \phi - v_r \cos \phi \quad (31).$$

$v_r$  and  $v_\theta$  can be expressed as

$$v_r = e \sqrt{\frac{\gamma}{l}} \sin f, v_\theta = \sqrt{\frac{\gamma}{l}} (1 + e \cos f) \quad (32),$$

$\gamma$  being the constant where  $\gamma/r^2$  is the magnitude of the attraction per unit mass a distance  $r$  from the attracting body. Equation 32 allows equation 31 to become

$$e \sin f = \frac{l}{r} \tan \phi - W \sqrt{\frac{l}{\gamma}} \sec \phi \quad (33).$$

If the orbit being transferred to is described by  $l'$ ,  $e'$ ,  $\omega'$ , then

$$e' \sin f' = \frac{l'}{r} \tan \phi - W \sqrt{\frac{l'}{\gamma}} \sec \phi \quad (34).$$

Of course the primer,  $\mathbf{p}$ , and its derivative,  $\dot{\mathbf{p}}$  are continuous across the junction point. From equations 27-30, it follows that

$$\left. \begin{aligned} A' \cos f' + B'e' \sin f' &= A \cos f + B e \sin f = \sin \phi, \\ -A' \sin f' + B'(1 + e' \cos f') + \frac{D' - A' \sin f'}{1 + e' \cos f'} &= \\ -A \sin f + B(1 + e \cos f) + \frac{D - A \sin f}{1 + e \cos f} &= \cos \phi, \\ l'^{1/2} \left( \frac{A' \sin f' - D'}{1 + e' \cos f'} - B' \right) &= l^{1/2} \left( \frac{A \sin f - D}{1 + e \cos f} - B \right), \\ l'^{-3/2} [-A'(e' + \cos f') + D'e' \sin f'] &= l^{-3/2} [-A(e + \cos f) + D e \sin f]. \end{aligned} \right\} (35).$$

These are sufficient for finding  $A, B, D, A', B', D'$ . Equations 35 can be reduced to

$$\left. \begin{aligned} e \sqrt{\frac{\gamma}{l}} A &= W - \frac{\gamma}{Wr} \sin^2 \phi \\ e^2 B &= \left( \frac{l}{r} - 1 \right) \left( 1 + \frac{\gamma^{1/2}}{Wl^{1/2}} \sin \phi \right) \cos \phi + \left( \frac{l}{r} \sin \phi - \frac{Wl^{1/2}}{\gamma^{1/2}} \right) \tan \phi \\ B + D &= - \left[ 1 + \frac{\gamma^{1/2}}{Wl^{1/2}} \left( \frac{l}{r} + 1 \right) \sin \phi \right] \cos \phi \end{aligned} \right\} (36).$$

Once  $A, B,$  and  $D$  are calculated from equations 36, the primer is determined over the orbit  $(l, e, \omega)$ . When equations 36 are calculated with primed quantities  $A', B', D', l'$ , and  $e'$  the primer will be determined over the second orbit  $(l', e', \omega')$ .

The characteristic velocity,  $V$ , for this maneuver is simply the difference in velocity at point  $P$  between the first and second orbit. Referring to figure 1, if the

component of spacecraft velocity in the direction of thrust  $T$  is denoted as  $U$  for the orbit  $(l, e, \omega)$  then

$$v_{\theta} = U \cos \phi + W \sin \phi \quad (37)$$

and

$$U = \frac{\sqrt{\gamma l}}{r} \sec \phi - W \tan \phi \quad (38).$$

Similarly for  $U'$  in orbit  $(l', e', \omega')$ ,

$$U' = \frac{\sqrt{\gamma l'}}{r} \sec \phi - W \tan \phi \quad (39).$$

Subtracting equation 39 from 38 yields the characteristic velocity as

$$V = U - U' = \frac{\gamma^{1/2}}{r} (l^{1/2} - l'^{1/2}) \sec \phi \quad (40).$$

### ***Two-Impulse Transfers***

If there are two coplanar orbits  $(l_1, e_1, \omega_1)$  and  $(l_2, e_2, \omega_2)$ , a transfer can be performed from the first orbit to the second with two impulses. In this case an intermediate transfer orbit, described by  $(l, e, \omega)$ , will exist between these two terminal orbits. The transfer orbit intersects the terminal orbits at junctions  $P_1$  and  $P_2$  respectively. Similar to the single impulse case in figure 1, polar coordinates for  $P_i$  ( $i=1, 2$ ) are  $(r_i, \theta_i)$ . The angle between the perpendicular to the radius vector and the impulse thrust will be denoted as  $\phi_i$  and  $W_i$  is the velocity component perpendicular to the impulse<sup>2</sup>.

Since the constants  $A, B, D$  in equations 27-30 will have the same value over the entire transfer orbit, calculating these at  $P_1$  or  $P_2$  will achieve the same result. Therefore three conditions for the transfer orbit can be derived from equations 36. These conditions will allow the 3 orbital elements to be determined. Let  $p, q, s_i, Z_i$  be defined as follows

$$p = \frac{1}{l}, q = \frac{e}{l} \quad (41),$$

$$s_i = \frac{1}{r_i}, Z_i = \frac{W_i}{(\gamma^{1/2} \sin \phi_i)} \quad (42).$$

The three conditions can now be expressed as

$$\left. \begin{aligned} & \left( Z_1 - \frac{s_1}{Z_1} \right) \sin \phi_1 = \left( Z_2 - \frac{s_2}{Z_2} \right) \sin \phi_2 \\ & (s_1 - p) \left( 1 + \frac{p^{1/2}}{Z_1} \right) \cos \phi_1 + (s_1 - Z_1 p^{1/2}) \sin \phi_1 \tan \phi_1 = \\ & (s_2 - p) \left( 1 + \frac{p^{1/2}}{Z_2} \right) \cos \phi_2 + (s_2 - Z_2 p^{1/2}) \sin \phi_2 \tan \phi_2 \\ & \left( 1 + \frac{s_1 + p}{Z_1 p^{1/2}} \right) \cos \phi_1 = \left( 1 + \frac{s_2 + p}{Z_2 p^{1/2}} \right) \cos \phi_2 \end{aligned} \right\} \quad (43).$$

To determine the optimal transfer orbit  $s_i$ ,  $\theta_i$ ,  $Z_i$ ,  $\phi_i$  need to be related to the orbital elements. Knowing from orbital mechanics that  $\frac{l}{r} = 1 + e \cos f$  and  $f = \theta - \omega$  the

following can be written:

$$\left. \begin{aligned} q_1 \cos(\theta_1 - \omega_1) &= s_1 - p_1, \\ q \cos(\theta_1 - \omega) &= s_1 - p, \\ q \cos(\theta_2 - \omega) &= s_2 - p, \\ q_2 \cos(\theta_2 - \omega_2) &= s_2 - p_2, \end{aligned} \right\} \quad (44).$$

At both junction points  $W_i$  will remain constant across the junction. Therefore, there are two equations like equation 33 at each junction. In the new notation these four equations can be written as

$$\left. \begin{aligned}
 q_1 \sin(\theta_1 - \omega_1) &= (s_1 - p_1^{1/2} Z_1) \tan \phi_1, \\
 q \sin(\theta_1 - \omega) &= (s_1 - p^{1/2} Z_1) \tan \phi_1, \\
 q \sin(\theta_2 - \omega) &= (s_2 - p^{1/2} Z_2) \tan \phi_2, \\
 q_2 \sin(\theta_2 - \omega_2) &= (s_2 - p_2^{1/2} Z_2) \tan \phi_2,
 \end{aligned} \right\} (45).$$

Equations 43-45 now provide eleven equations to solve the eleven unknowns ( $s_1, s_2, \theta_1, \theta_2, Z_1, Z_2, \phi_1, \phi_2, p, q, \omega$ ). The last three unknowns through equation 41 will describe the optimal transfer orbit ( $l, e, \omega$ ).

### Rotation of Orbit Axes

Consider the more specific case of transfer between coplanar ellipses of identical size and shape, as shown in figure 2. The effect of this transfer is to rotate the major axis of orbit 1 described by ( $P, Q, -\alpha$ ) through an angle of  $2\alpha$  to orbit 2 described by ( $P, Q, \alpha$ ).

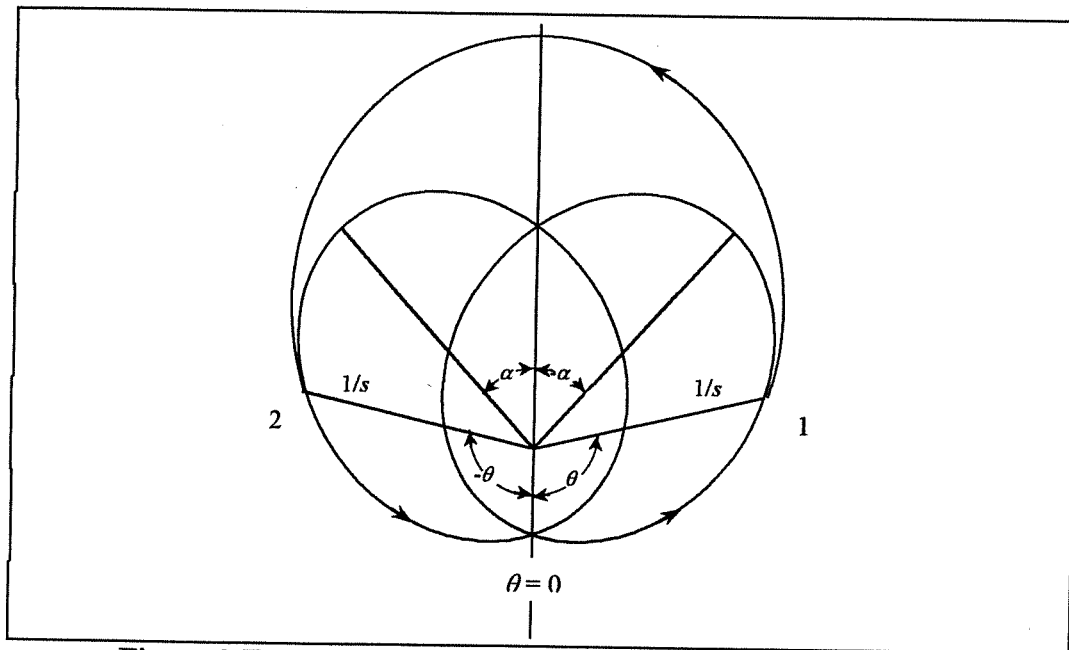


Figure 2 Two-impulse transfer between identical ellipses

Since there is an obvious symmetry across the line where  $\theta = 0$ , the transfer orbit will be assumed to have its major axis along this line and will be described by  $(p, q, 0)$ . The junction points for this transfer ellipse will then be at polar coordinates  $(1/s, \theta)$  and  $(1/s, -\theta)$ . Due to the symmetry of this case it is clear that  $Z$ , given by equation 42, will have the same value at both junction points. Also, if  $\phi$  determines the direction of the thrust at junction 1, then  $\pi - \phi$  determines the direction at junction 2. This means that equations 44 and 45 are reduced to

$$\left. \begin{aligned} Q \cos(\theta + \alpha) &= s - P, \\ Q \sin(\theta + \alpha) &= (s - Zp^{1/2}) \tan \phi, \\ q \cos \theta &= s - p, \\ q \sin \theta &= (s - Zp^{1/2}) \tan \phi, \end{aligned} \right\} (46)$$

and equation 43 reduces to

$$\left. \begin{aligned} (s - p) \left( 1 + \frac{p^{1/2}}{Z} \right) \cos \phi + (s - Zp^{1/2}) \sin \phi \tan \phi &= 0, \\ \left( 1 + \frac{s + p}{Zp^{1/2}} \right) \cos \phi &= 0 \end{aligned} \right\} (47).$$

The six conditions contained in equations 46 and 47 determine the six unknowns  $p, q, s, \theta, Z, \phi$ .

To avoid  $\tan \phi$  going to infinity, the possibility of  $\cos \phi = 0$  is rejected. Then by equation 47

$$\frac{Z}{p^{1/2}} = -\frac{(x+1)}{x} \quad (48)$$

where  $x$  is defined as

$$x = \frac{p}{s} = \frac{r}{l} \quad (49).$$

Substituting equation 49 into equation 47 yields

$$\tan^2 \phi = \frac{x-1}{(x+1)(x+2)} \quad (50)$$

which shows that  $x \geq 1$ . If  $E = Q/P$  is the eccentricity of the terminal orbits and  $e = q/p$  is the eccentricity of the transfer ellipse, equation 46 can be written as

$$\left. \begin{aligned} e \cos \theta &= \frac{1}{x} - 1, \\ e \sin \theta &= \frac{x+2}{x} \tan \phi, \\ E \cos(\theta + \alpha) &= \frac{y^2}{x} - 1, \\ E \sin(\theta + \alpha) &= \frac{y(x+y+1)}{x} \tan \phi \end{aligned} \right\} (51).$$

Here  $y = \sqrt{P/p}$ . Dividing the fourth of these equations by the third gives

$$\tan(\theta + \alpha) = \frac{y(x+y+1)}{y^2 - x} \tan \phi \quad (52).$$

When  $E$  and  $a$  are known, equations 50 and 51 can determine  $x, y, e, \theta, \phi$ . From equation 40, the characteristic velocity can be found to be  $\gamma^{1/2} X$ , where

$$XP^{-1/2} = \frac{2}{x}(1-y)y \sec \phi \quad (53).$$

It can be assumed that  $\alpha$  lies in the range  $0 \leq \alpha \leq \pi/2$ . Since the angle between the orbits is  $2\alpha$ , a value of  $\alpha$  outside this range can be forced inside the range by changing the perspective of the problem. Equations 50 and 51 can be solved by assuming values for  $x$  and  $y$  and determining the corresponding value of  $\phi$  from equation 50. This must be done in a manner that maintains a positive value for  $X$  in equation 53. This restricts  $\phi$  to lie within two quadrants but the sign of  $\tan \phi$  is still undetermined. For each sign of  $\tan \phi$  equation 51 has a value for  $\tan \theta$ , and therefore two values of  $\theta$  with a difference of  $\pi$ . In equation 52, only two of these values will keep  $\alpha$  within its range. Only one of these two values will produce a positive value for  $E$  in equation 51.

Figure 3<sup>2</sup> shows calculations for  $XP^{1/2}$  for selected values of  $E$  across the range of valid  $\alpha$ . From this it is seen that a maximum propellant expenditure occurs when  $\alpha = 90^\circ$ . For a given  $a$ , this maximum occurs when  $0.7 < E < 0.8$ .

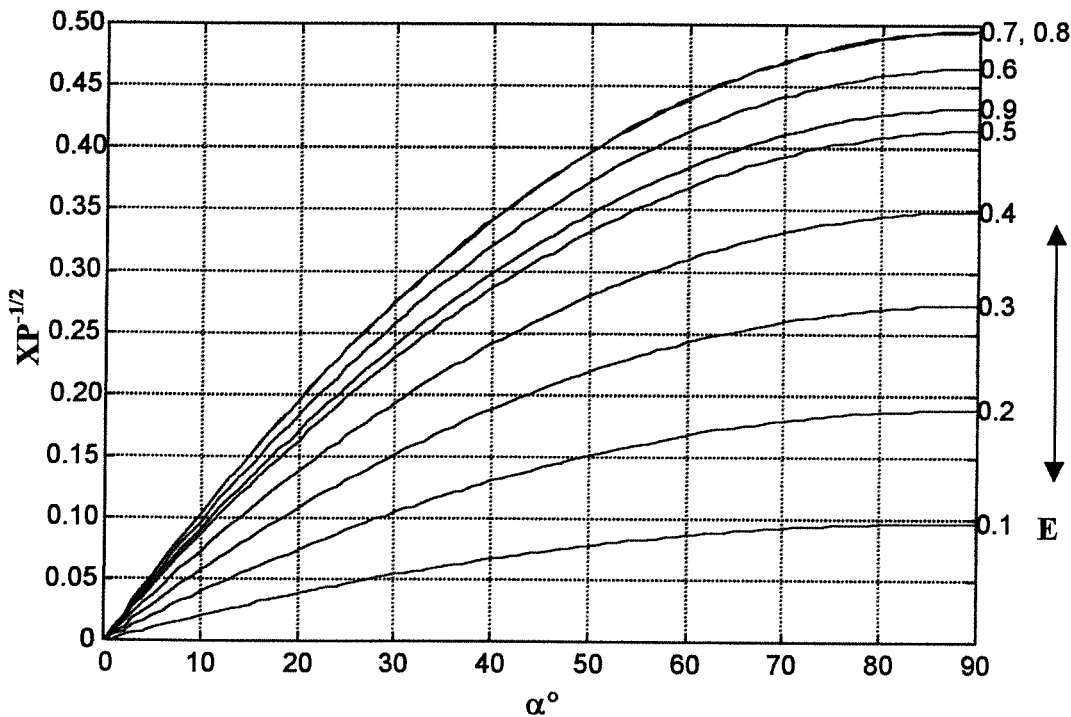


Figure 3 Characteristic velocity for orbit rotation

## Circular Orbits

The optimal transfer between two circular, concentric, coplanar orbits is generally considered to be the Hohmann transfer. This transfer, as shown in figure 4, is performed along an ellipse with apses located on the two circles. At the locations of these apses velocity is completely tangential to both orbits, therefore the thrust has only to change the magnitude of the velocity.

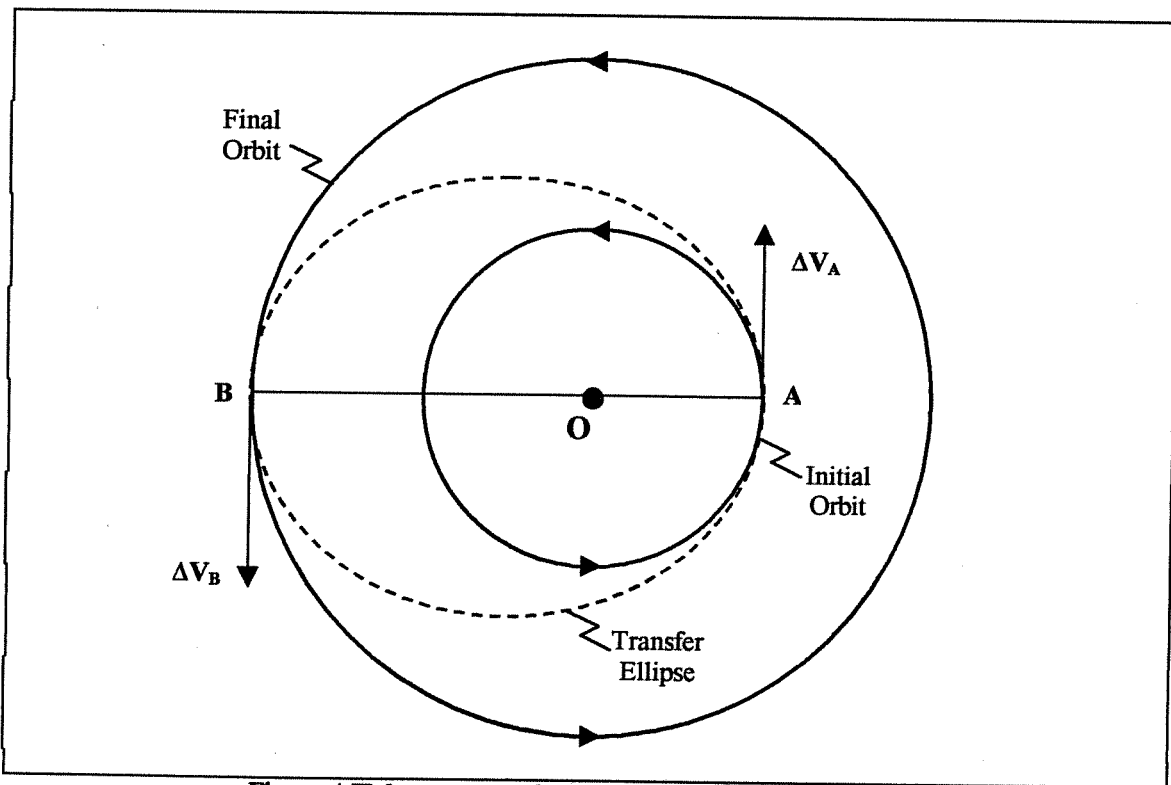


Figure 4 Hohmann transfer raising the orbit altitude

Since the thrust is purely tangential, the primer in polar coordinates will have one component as will its derivative. The derivatives are determined by Lawden<sup>1</sup> for a circle of radius  $a$  as

$$\xi = -\frac{\gamma^{1/2}}{2a^{3/2}}(P + D) \quad (54),$$

for an ellipse at  $f = 0$  as

$$\xi = -\frac{\gamma^{1/2}}{2l^{3/2}} P(1+e)^2(2-e) \quad (55),$$

and an ellipse at  $f = \pi$  as

$$\xi = -\frac{\gamma^{1/2}}{2l^{3/2}} P(1-e)^2(2+e) \quad (56).$$

$P$  is the magnitude of the primer and  $D$  is a constant. These equations assume that the thrust is applied in the direction of motion. If the thrust opposes the motion, the sign of  $\xi$  will be reversed.

Let orbits A and B in figure 4 have radii  $a$  and  $b$  respectively. Taking  $P = 1$ , and applying the condition that  $\dot{\mathbf{p}}$  is a constant over a junction point to point A yields

$$D+1 = \left(\frac{a}{l}\right)^{3/2} (1+e)^2(2-e) \quad (57).$$

It can be seen from figure 4 that

$$a = \frac{l}{(1+e)} \quad (58)$$

and equation 57 becomes

$$D+1 = (1+e)^{1/2}(2-e) \quad (59).$$

Applying equations 54 and 56 at point B in a similar manner finds

$$D'+1 = (1-e)^{1/2}(2+e) \quad (60).$$

Since  $D$  and  $D'$  must take values between 0 and 1 for an optimal transfer<sup>1</sup>. Equations 59 and 60 respectively become

$$1 \leq (1+e)^{1/2}(2-e) \leq 2, \quad (61),$$

$$1 \leq (1-e)^{1/2}(2+e) \leq 2 \quad (62).$$

Figure 5 shows the function

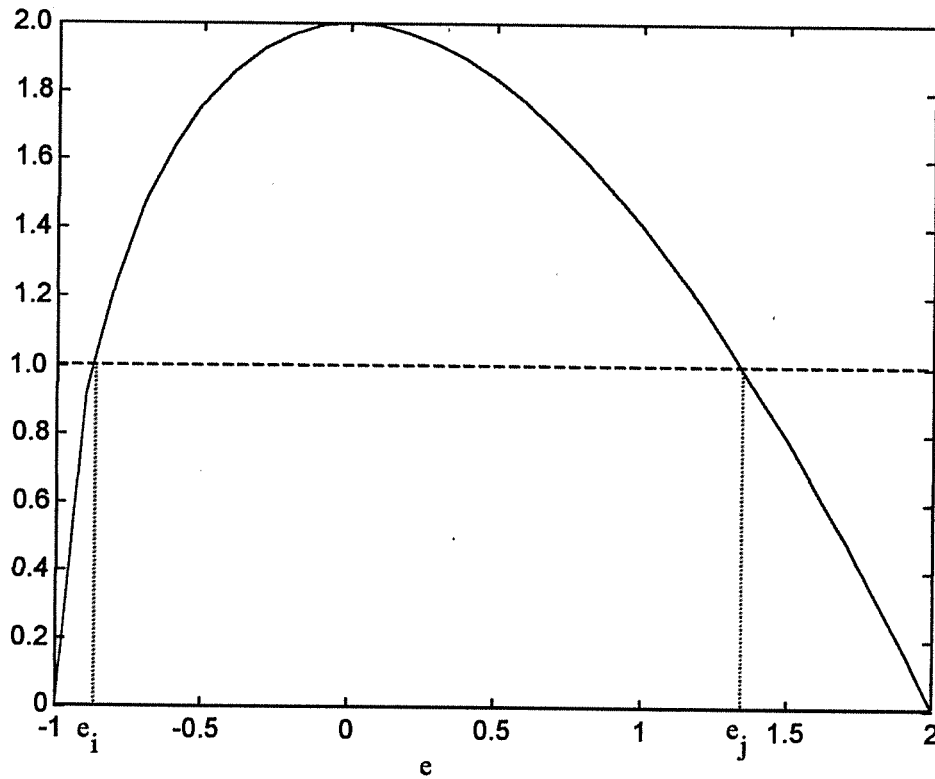


Figure 5 Possible eccentricities for transfer ellipse

$$y = (1+e)^{1/2}(2-e) \quad (63).$$

Here it can be seen that equation 61 will be satisfied when  $e$  has a value between  $e_i$  and  $e_j$ .

$-e_i, e_j$  are the roots to

$$x^3 - 3x^2 + 3 = 0 \quad (64)$$

and are found as  $e_i = 0.8794$  and  $e_j = 1.3473$ . Similar analysis for equation 62 produces a mirror image of figure 5. To satisfy both conditions,  $e$  must have a value

$$0 \leq e \leq 0.8794 \quad (65).$$

If  $a_t$  is the semi-major axis of the transfer ellipse then

$$a = a_t(1-e), b = a_t(1+e) \quad (66).$$

Solving for  $a_t$  and  $e$  yields

$$a_t = \frac{1}{2}(a+b), e = \frac{\rho-1}{\rho+1} \quad (67),$$

where  $\rho = b/a$ . Applying the condition from equation 65 finds that

$$0 \leq \rho \leq 15.58 \quad (68).$$

So the Hohmann transfer can not be proved optimal for orbits whose ratio of radii exceeds 15.58. An optimal transfer for these cases can be found through a three impulse transfer.

### *Three-Impulse Transfers*

The characteristic velocity of the Hohmann transfer can be determined by summing the two velocity increments. When this sum is divided by the initial orbit velocity, denoted as  $c_1$ , the characteristic velocity becomes a dimensionless function of the radii of the terminal orbits and can be written as

$$\frac{\Delta v_t}{c_1} = \left(1 - \frac{1}{r_2/r_1}\right) \sqrt{\frac{2(r_2/r_1)}{1+(r_2/r_1)}} + \frac{1}{\sqrt{r_2/r_1}} - 1 \quad (69).$$

This function is plotted in figure 6 for a broad range of  $r_2/r_1$ . If instead of a Hohmann transfer, the spacecraft were sent on a Hohmann-like ellipse to infinity and returned likewise to the final orbit. Here instead of one half ellipse with apses on the terminal orbits, there are two half ellipses with a common apse at a third point in space, in this case infinity. Hoelker and Silber termed this a bi-elliptic transfer<sup>3</sup>. The velocity increments would now be the difference in circular and escape velocities for the terminal orbits. The characteristic velocity for this maneuver can be given as

$$\frac{(\Delta v_t)_\infty}{c_1} = (\sqrt{2} - 1) \left(1 + \frac{1}{\sqrt{r_2/r_1}}\right) \quad (70)$$

and is also plotted in figure 6.

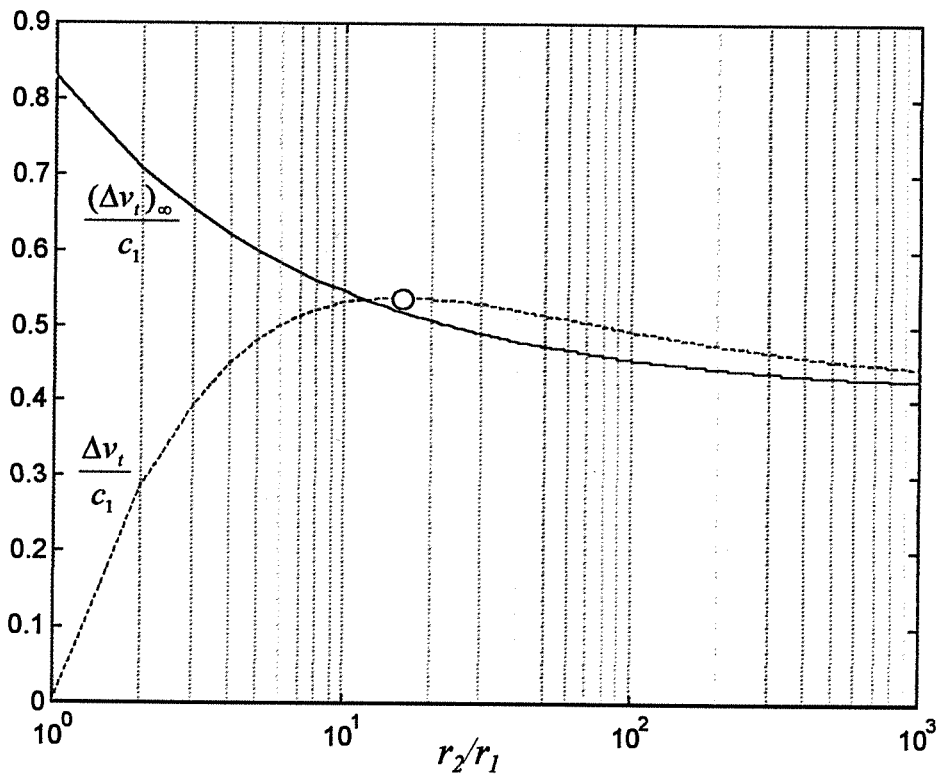


Figure 6 Characteristic velocity for Hohmann and bi-elliptic transfers

From this figure it is evident that the characteristic velocities are equal when the ratio is 11.94. For larger ratios, the characteristic velocity is smaller for the bi-elliptic method.

Figure 7, shows a diagram of this method. The distance to the intermediate point will now be designated as  $r_2$ , the final orbit radius as  $r_3$ , and the terminal ratio as  $r_3/r_1$ . The ratio  $r_2/r_1$  is called the conjunction ratio. There are three different types of bi-elliptic transfers. The first occurs when  $r_2/r_1 \geq r_3/r_1 > 1$ , this is called an exterior conjunction. The other two are called interior conjunctions. One occurs when  $r_3/r_1 \geq r_2/r_1 > 1$  and the other when  $r_3/r_1 > 1 > r_2/r_1^3$ .

For the first type of bi-elliptical transfer, the characteristic velocity can be given by

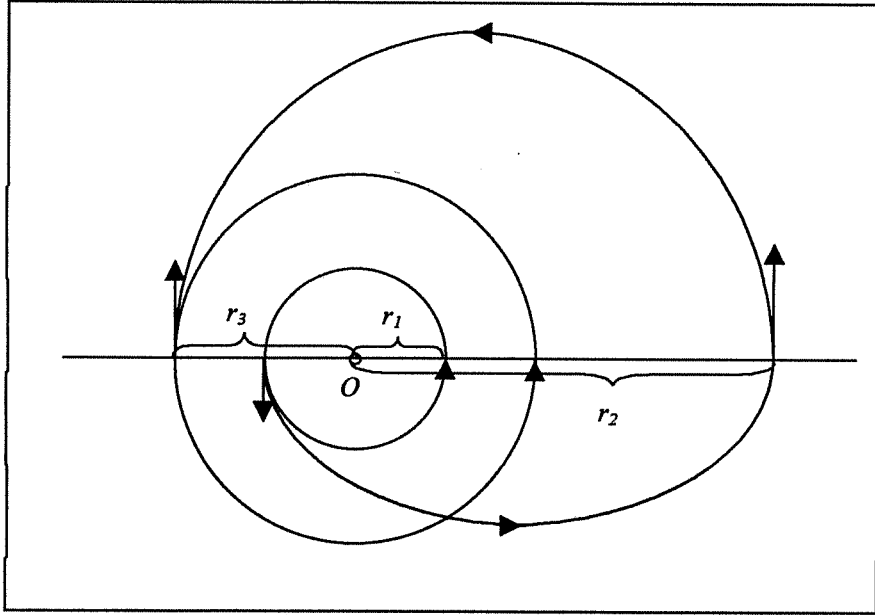


Figure 7 Bi-elliptic transfer with exterior conjunction

$$\frac{\Delta v_t}{c_1} = \sqrt{\frac{2(r_3/r_1)}{1+(r_2/r_1)}} - 1 + \sqrt{\frac{2}{r_2/r_1}} \left( \sqrt{\frac{1}{1+(r_2/r_1)/(r_3/r_1)}} - \sqrt{\frac{1}{1+(r_2/r_1)}} \right) + \sqrt{\frac{1}{r_3/r_1}} \left( \sqrt{\frac{2(r_2/r_1)}{(r_2/r_1)+(r_3/r_1)}} - 1 \right) \quad (71).$$

Equation 71 is plotted in figure 8 as a function of the conjunction ratio for various terminal ratios. The broken line in this figure represents the Hohmann transfer ( $r_2/r_1 = r_3/r_1$ ). Each parametric curve begins on this line. Figure 8 shows that for some terminal ratios, the characteristic velocity decreases with increased conjunction ratio. Therefore, some bi-elliptical transfers are more economical than Hohmann transfers. Further investigation would show that any of these parametric curves that has a negative slope at the first point would achieve a smaller characteristic velocity than the Hohmann transfer. The slope at this point can be determined by differentiating equation 71 with respect to the conjunction ratio and equating the conjunction and terminal ratios<sup>3</sup>. This yields

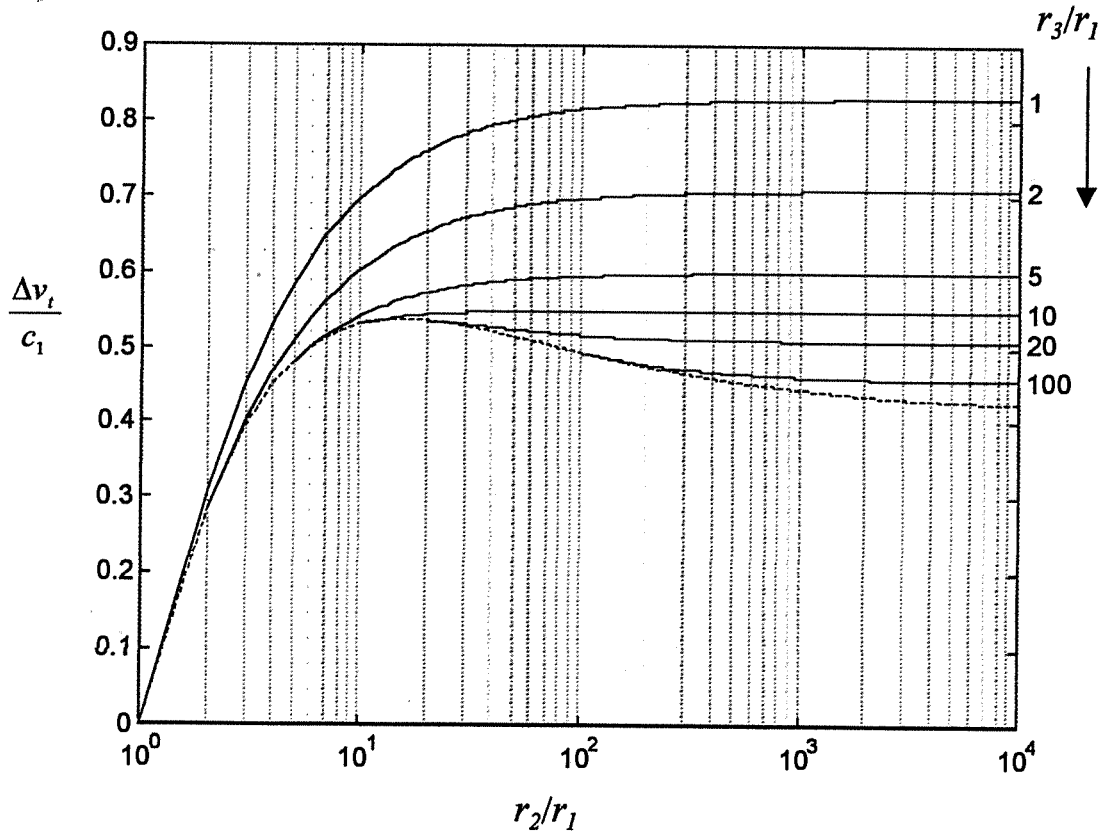
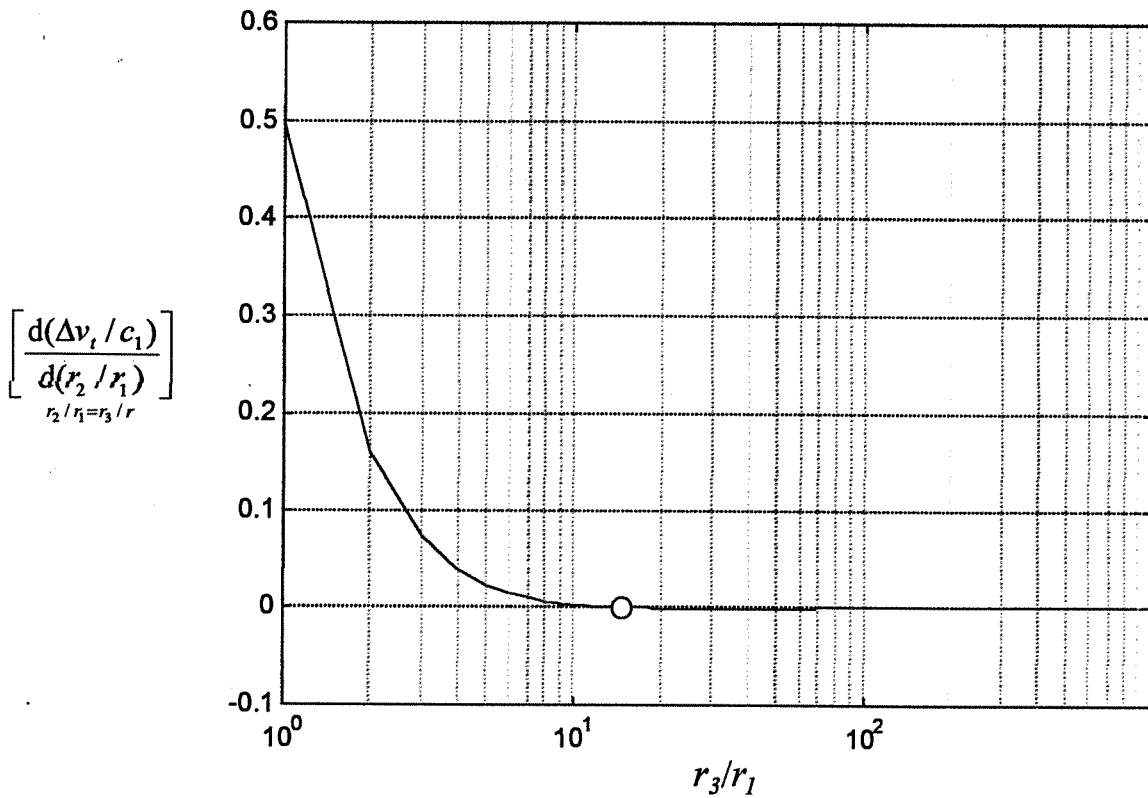


Figure 8 Characteristic velocity for exterior conjunction bi-elliptic transfer  
(the broken line represents a Hohmann transfer)

$$\left[ \frac{d(\Delta v_t / c_1)}{d(r_2 / r_1)} \right]_{r_2/r_1=r_3/r_1} = \frac{\sqrt{2}}{(r_3 / r_1)^2} \left[ \frac{1}{\sqrt{1 + \left( \frac{1}{r_3 / r_1} \right)}} + \frac{1 - \left( \frac{1}{r_3 / r_1} \right)}{2 \left[ 1 + \left( \frac{1}{r_3 / r_1} \right) \right]^{3/2}} - \frac{1}{2 \sqrt{2 / (r_3 / r_1)}} \right] \quad (72).$$

This is plotted in figure 9, where it can be seen that negative values are obtained for terminal ratios greater than  $\sim 15.58$ . This is the same value presented in the previous section and is denoted as  $\rho_{\text{crit}}$ . Therefore, all bi-elliptic transfers with a terminal ratio greater than or equal to  $\rho_{\text{crit}}$  are more economical than a Hohmann transfer with the same terminal ratio.



**Figure 9 Derivative of characteristic velocity for exterior conjunction bi-elliptic transfer**

If the derivative of equation 71 is set to zero and solved for the conjunction ratio, then

$$r_2 / r_1 = - \frac{3 + \left( \frac{1}{(r_3 / r_1)} \right)}{3 \left[ 1 + \left( \frac{1}{(r_3 / r_1)} \right) \right] - 2 \sqrt{3 - \left( \frac{2}{(r_3 / r_1)} \right)}} \quad (73).$$

By equation 73,  $r_2/r_1$  is undefined when  $r_3/r_1 = 9$  and is negative for  $r_3/r_1 < 9$ . For these values the slope of the curves is positive and remains positive. Therefore bi-elliptic transfers with conjunction ratios less than 9 are less economical than Hohmann transfers. For  $9 < r_3/r_1 < \rho_{crit+}$ , the parametric curves contain one maximum and decrease as the conjunction ratio increases to infinity<sup>3</sup>. To determine if the characteristic velocity decreases to a value less than that of the Hohmann transfer, the two must be equal in value for a conjunction ratio other than one equal to the terminal ratio. Setting equations

69 and 71 equal produces the following

$$\frac{1-r_2/r_1}{\sqrt{(r_2/r_1)(1+r_2/r_1)}} - \frac{1-r_3/r_1}{\sqrt{(r_3/r_1)(1+r_3/r_1)}} - \sqrt{\left(\frac{1}{r_2/r_1} + \frac{1}{r_3/r_1}\right)} + \sqrt{\frac{2}{r_3/r_1}} = 0 \quad (74).$$

This has the solution

$$r_2/r_1 = \frac{A + \sqrt{B}}{2} \quad (75a)$$

where,

$$\left. \begin{aligned} B &= A^2 - \frac{4}{(r_3/r_1)[(M+R)^2 - 1]}, \\ A &= \frac{1}{(r_3/r_1)} \left[ \frac{(M-3R)^2 + 1}{(M+R)^2 - 1} + \frac{1}{(r_3/r_1)} \left( \frac{1}{1-(M+R)^2} \right) \right], \\ M &= R \left( K^2 - \frac{1}{(r_3/r_1)} \right), \\ R &= \frac{1}{2K}, \\ K &= \frac{(r_3/r_1) - 1}{(r_3/r_1)} \sqrt{\frac{(r_3/r_1)}{1+(r_3/r_1)}} + \sqrt{\frac{2}{(r_3/r_1)}}. \end{aligned} \right\} (76b).$$

This solution is shown graphically in figure 10. This figure shows that for a terminal ratio  $\rho_{\text{crit}}$ , the conjunction ratio will have a value of  $\rho_{\text{crit}}$ . It also shows that the conjunction ratio is infinite for a terminal ratio equal to some  $\rho_f$  (feasibility ratio). This ratio can be defined as the largest positive root of

$$x^3 - (7 + 4\sqrt{2})x^2 + (3 + 4\sqrt{2})x - 1.$$

This yields  $\rho_f \approx 11.939$ . Therefore, when  $\rho_f \leq r_3/r_1 \leq \rho_{\text{crit}}$ , the bi-elliptic transfer is more economical than the Hohmann transfer provided that the conjunction ratio is greater than or equal to some critical value given by equation 75<sup>3</sup>.

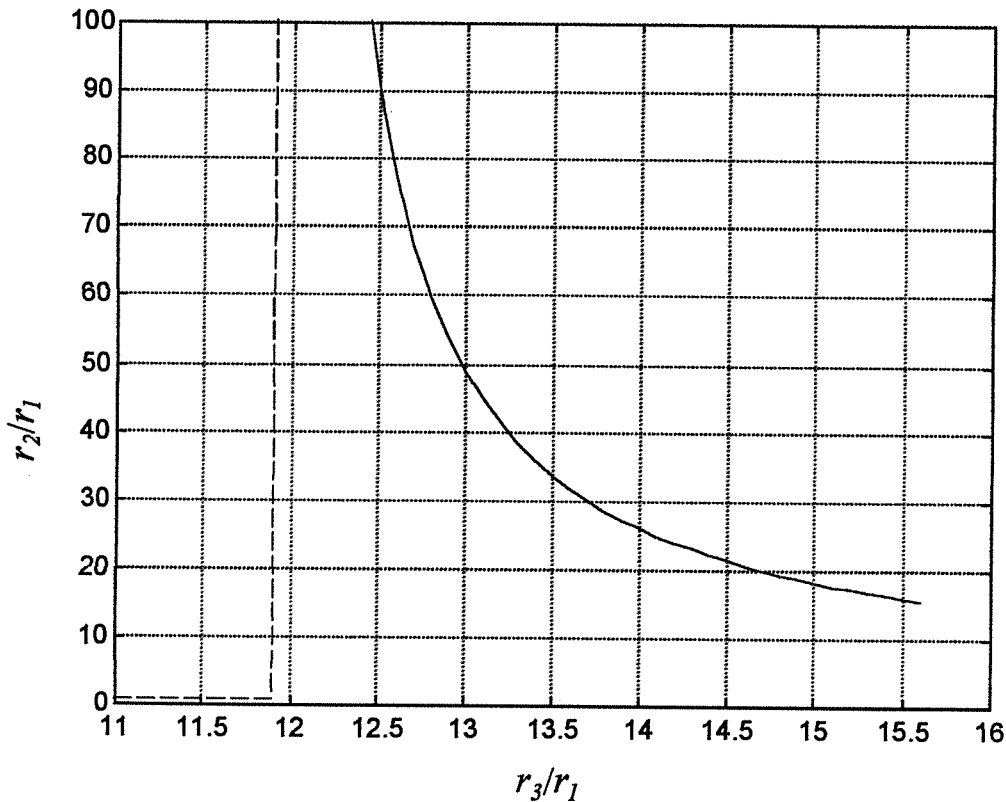


**Figure 10 Feasibility for  $9 < r_3/r_1 < \rho_{crit}$**

Figures 11 and 12 show the characteristic velocities for the two interior conjunction cases. Figure 11 clearly shows that the bi-elliptic transfer is never more economical than the Hohmann transfer for  $1 \leq r_2/r_1 \leq r_3/r_1$ . Figure 12 shows that the characteristic velocity increases with a decreasing conjunction ratio, offering little benefit in seeking a transfer orbit in this region.

The three impulse, bi-elliptic transfer is more economical for terminal ratios greater than 11.939. The characteristic velocity for these transfers approaches a minimum when the conjunction ratio is infinite. Since this corresponds to two half parabolas with no impulse needed at their conjunction, the addition of more than three impulses would probably not add any savings<sup>3</sup>.

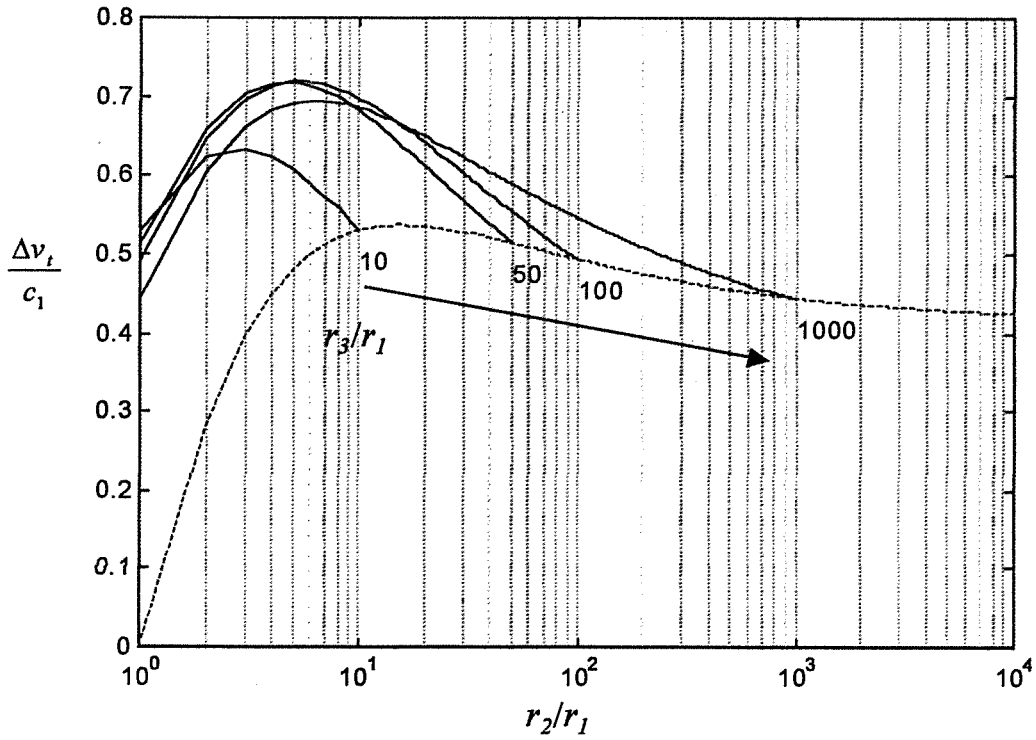


Figure 11 Characteristic velocity for  $1 \leq r_2/r_1 \leq r_3/r_1$   
 (the broken line represents the Hohmann transfer)

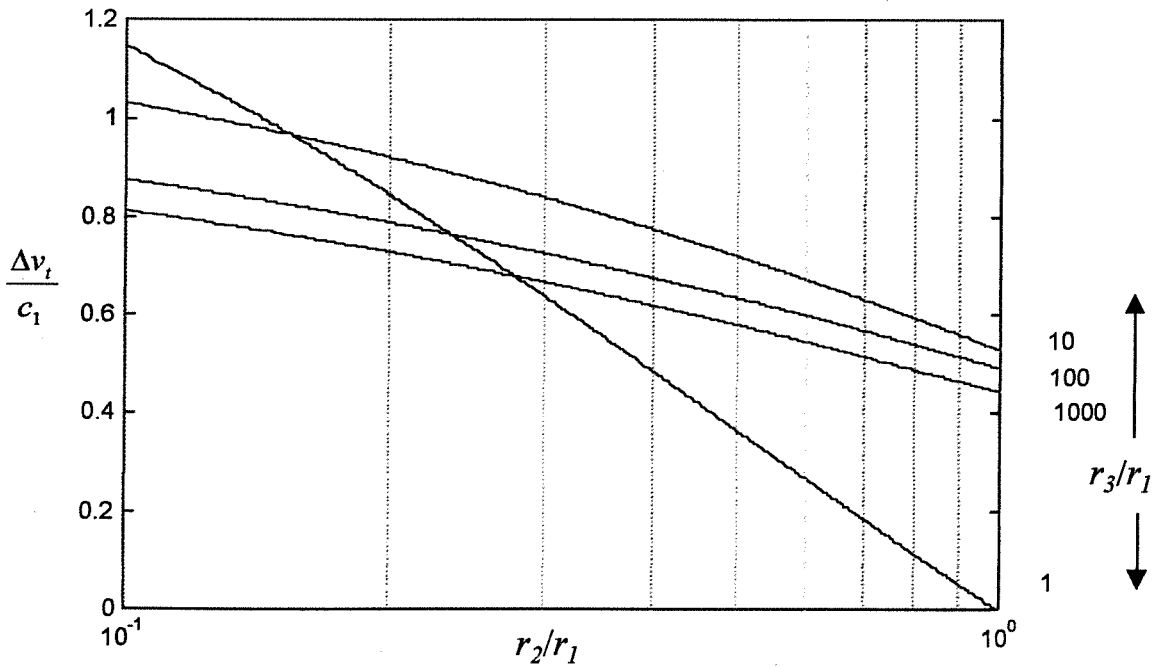


Figure 12 Characteristic velocity for  $r_2/r_1 < 1$

## N-Impulse Transfers

Lawden's one and two impulse transfers can be expanded to a case of n-impulses. For this case the transfers will take place between orbits described by  $(p_0, q_0, \omega_0)$  and  $(p_n, q_n, \omega_n)$ . The first impulse transfers the spacecraft from orbit  $(p_0, q_0, \omega_0)$  to  $(p_1, q_1, \omega_1)$  at point  $(1/s_1, \theta_1)$ , the second transfers from  $(p_1, q_1, \omega_1)$  to  $(p_2, q_2, \omega_2)$  at  $(1/s_2, \theta_2)$ , and so on to point  $(1/s_n, \theta_n)$ . At this point the  $n^{\text{th}}$  impulse places the spacecraft into orbit  $(p_n, q_n, \omega_n)^2$ . Let  $\gamma^{1/2} X_i$  be the characteristic velocity for the  $i^{\text{th}}$  impulse (similar to equation 53), and

$$X_i = s_i (p_i^{-1/2} - p_{i-1}^{-1/2}) \sec \phi_i \quad (77),$$

where  $\phi_i$  is the angle of the thrust direction. Then the total characteristic velocity for the maneuver is

$$V_{tot} = \gamma^{1/2} \sum_{i=1}^n X_i \quad (78).$$

Since  $X_i$  is a function of the six parameters  $(p_{i-1}, q_{i-1}, \omega_{i-1}, p_i, q_i, \omega_i)$ ,  $V_{tot}$  is a function of  $3n-3$  variables  $(p_1, q_1, \omega_1, \dots, p_n, q_n, \omega_n)$ .  $V_{tot}$  is stationary with respect to these arguments if for  $i=1, 2, \dots, (n-1)$

$$\frac{\partial V_{tot}}{\partial p_i} = \frac{\partial V_{tot}}{\partial q_i} = \frac{\partial V_{tot}}{\partial \omega_i} = 0 \quad (79).$$

The parameters  $(p_i, q_i, \omega_i)$  for the optimal n-impulse transfer must satisfy equations 78.

By solving these, and computing a value for  $V_{tot}$ , the optimal transfer should be determined.

Now,

$$\frac{\partial V_{tot}}{\partial p_i} = \gamma^{1/2} \left( \frac{\partial X_i}{\partial p_i} + \frac{\partial X_{i+1}}{\partial p_i} \right) \quad (80),$$

$$\left. \begin{aligned} \frac{\partial X_i}{\partial p_i} &= \frac{\partial s_i}{\partial p_i} (p_{i+1}^{-1/2} - p_i^{-1/2}) \sec \phi_i + \frac{1}{2} s_i p_i^{-3/2} \sec \phi_i \\ &\quad + s_i (p_{i+1}^{-1/2} - p_i^{-1/2}) \sec \phi_i \tan \phi_i \frac{\partial \phi_i}{\partial p_i}, \\ \frac{\partial s_i}{\partial p_i} &= \frac{s_i - Z_i p_{i+1}^{1/2}}{Z_i (p_i^{1/2} - p_{i+1}^{1/2})}, \\ \frac{\partial \theta_i}{\partial p_i} &= \frac{\cot \phi_i}{Z_i (p_{i+1}^{1/2} - p_i^{1/2})}, \end{aligned} \right\} \quad (81),$$

Combining equations 80 yields

$$\frac{\partial X_i}{\partial p_i} = - \left[ \frac{s_i}{2 p_i^{3/2}} \sec^2 \phi_i - \frac{Z_i}{2 p_i} \tan^2 \phi_i - \frac{1}{p_i^{1/2}} - \frac{1}{Z_i} \right] \cos \phi_i \quad (82).$$

Found in a similar manner

$$\frac{\partial X_{i+1}}{\partial p_i} = \left[ \frac{s_{i+1}}{2 p_i^{3/2}} \sec^2 \phi_{i+1} - \frac{Z_{i+1}}{2 p_i} \tan^2 \phi_{i+1} - \frac{1}{p_i^{1/2}} - \frac{1}{Z_{i+1}} \right] \cos \phi_{i+1} \quad (83)$$

with similar equations for  $\frac{\partial V_{tot}}{\partial q_i}$  and  $\frac{\partial V_{tot}}{\partial \omega_i}$ .

$\frac{\partial V_{tot}}{\partial p_i}$  vanishes when

$$\left[ \frac{s_i}{2 p_i^{3/2}} \sec^2 \phi_i - \frac{Z_i}{2 p_i} \tan^2 \phi_i - \frac{1}{p_i^{1/2}} - \frac{1}{Z_i} \right] \cos \phi_i = \left[ \frac{s_{i+1}}{2 p_i^{3/2}} \sec^2 \phi_{i+1} - \frac{Z_{i+1}}{2 p_i} \tan^2 \phi_{i+1} - \frac{1}{p_i^{1/2}} - \frac{1}{Z_{i+1}} \right] \cos \phi_{i+1} \quad (84).$$

$\frac{\partial V_{tot}}{\partial q_i}$  and  $\frac{\partial V_{tot}}{\partial \omega_i}$  vanish when

$$\left. \begin{aligned} (s_i - p_i) \left( 1 + \frac{p_i^{1/2}}{Z_i} \right) \cos \phi_i + (s_i - p_i^{1/2} Z_i) \tan \phi_i \sin \phi_i = \\ (s_{i+1} - p_i) \left( 1 + \frac{p_i^{1/2}}{Z_{i+1}} \right) \cos \phi_{i+1} + (s_{i+1} - p_i^{1/2} Z_{i+1}) \tan \phi_{i+1} \sin \phi_{i+1} \end{aligned} \right\} (85),$$

$$\left( Z_i - \frac{s_i}{Z_i} \right) \sin \phi_i = \left( Z_{i+1} - \frac{s_{i+1}}{Z_{i+1}} \right) \sin \phi_{i+1} \quad (86).$$

The values of  $(s_i, \theta_i, Z_i, \phi_i)$  can be determined by

$$q_{i-1} \cos(\theta_i - \omega_{i-1}) = s_i - p_{i-1} \quad (87),$$

$$q_{i-1} \sin(\theta_i - \omega_{i-1}) = (s_i - Z_i p_{i-1}^{1/2}) \tan \phi_i \quad (88),$$

$$q_i \cos(\theta_i - \omega_i) = s_i - p_i \quad (89),$$

$$q_i \sin(\theta_i - \omega_i) = (s_i - Z_i p_i^{1/2}) \tan \phi_i \quad (90).$$

For  $i = 1, 2, \dots, (n-1)$ , equations 83-89 provide  $7n-7$  equations to find  $7n-7$  unknowns,  $p_i, q_i, \omega_i, s_i, \theta_i, Z_i, \phi_i$ . These  $7n-7$  parameters will describe an optimal  $n$ -impulse transfer between  $(p_0, q_0, \omega_0)$  and  $(p_n, q_n, \omega_n)$ .

## Non-Coplanar

Non-coplanar transfers are needed when it is necessary to alter the orbital inclination by some angle  $\theta$ . Transfers of this kind can change only the inclination or can be used to change the orbit shape as well.

### *Hohmann Transfer with Split-Plane Change*

As for coplanar orbits, the optimal two-impulse transfer between two concentric circular orbits is the Hohmann transfer. Again, the first impulse places the spacecraft on

a transfer ellipse. In this non-coplanar case, however, a component of this impulse is directed outside of the orbit plane. This causes the transfer ellipse to have an inclination that differs from that of the initial orbit by angle  $\alpha_1$ . Likewise the second impulse imparts another inclination change,  $\alpha_2 = \theta - \alpha_1$ , when placing the spacecraft on the final orbit<sup>4</sup>. This is represented in figure 13.

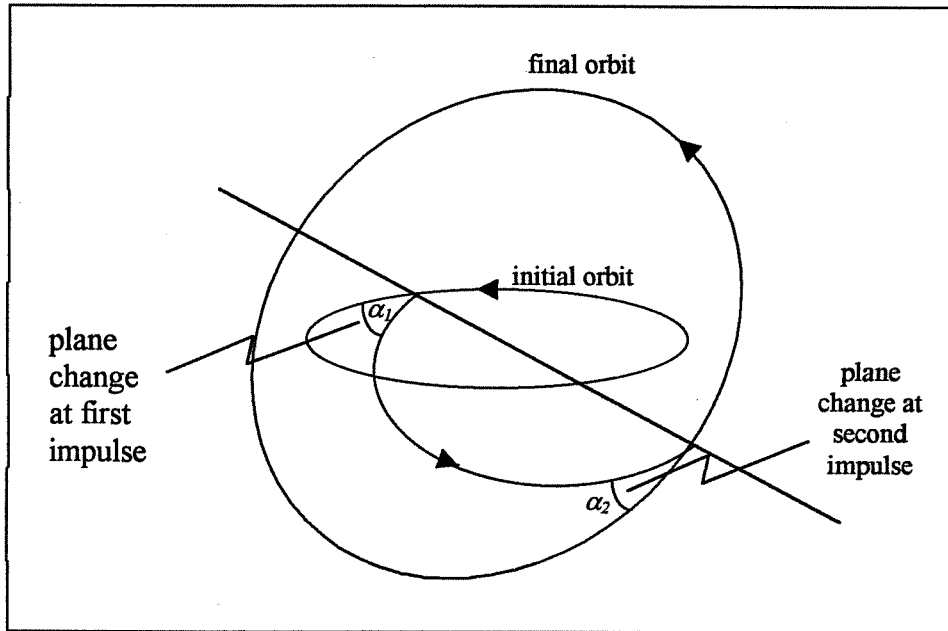


Figure 13 Hohmann transfer with split plane change

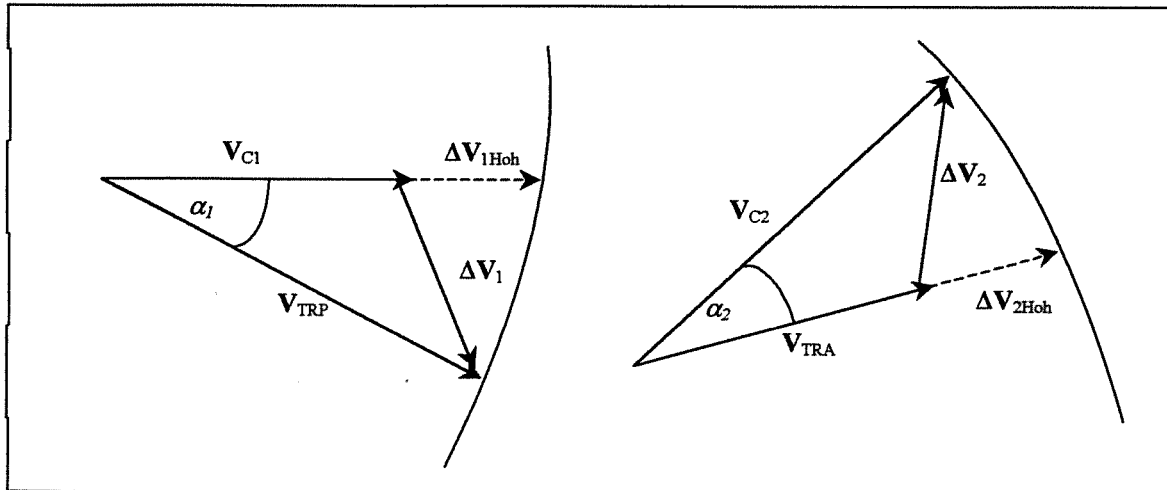


Figure 14 Velocity vector triangles for Hohmann plane change impulses

Figure 14 represents the vector addition triangles for the two impulses. Here,  $V_{c1}$  and  $V_{c2}$  are the circular velocities of the initial and final orbits respectively.  $\Delta V_{1Hoh}$  and  $\Delta V_{2Hoh}$  are the impulses for the coplanar version of this Hohmann transfer,  $\Delta V_1$  and  $\Delta V_2$  are the impulses for this non-coplanar transfer,  $V_{TRP}$  and  $V_{TRA}$  are the velocities at the perigee and apogee of the transfer ellipse, and  $\alpha_1$  and  $\alpha_2$  are the inclination changes at the impulses. Now

$$\Delta V_1^2 = V_{TRP}^2 + V_{c1}^2 = 2V_{TRP}V_{c1} \cos \alpha_1 \quad (91),$$

$$V_{TRP} = V_{c1} + \Delta V_{1Hoh} \quad (92),$$

$$V_{TRA} = V_{c2} + \Delta V_{2Hoh} \quad (93),$$

$$\Delta V_2^2 = V_{TRA}^2 + V_{c2}^2 = 2V_{TRA}V_{c2} \cos(\theta - \alpha_1) \quad (94),$$

$$\theta = \alpha_1 + \alpha_2 \quad (95),$$

$$\Delta V_{Tot} = \Delta V_1 + \Delta V_2 \quad (96).$$

To minimize  $\Delta V_{Tot}$ ,  $\frac{\partial \Delta V_{Tot}}{\partial \alpha_1}$  is set equal to zero.

$$\frac{\partial \Delta V_{Tot}}{\partial \alpha_1} = \frac{V_{TRP}V_{c1} \sin \alpha_1}{\Delta V_1} - \frac{V_{TRA}V_{c2} \sin(\theta - \alpha_1)}{\Delta V_2} = 0 \quad (97)$$

which leads to

$$\frac{V_{TRP}V_{c1} \sin \alpha_1}{\sqrt{V_{TRP}^2 + V_{c1}^2 - 2V_{TRP}V_{c1} \cos \alpha_1}} = \frac{V_{TRA}V_{c2} \sin(\theta - \alpha_1)}{\sqrt{V_{TRA}^2 + V_{c2}^2 - 2V_{TRA}V_{c2} \cos(\theta - \alpha_1)}} \quad (98).$$

Equation 97 can be solved iteratively to obtain  $\alpha_{1opt}$  then  $\alpha_{2opt} = \theta - \alpha_{1opt}$ . These can be substituted into equations 90 and 93 to obtain  $\Delta V_{1opt}$  and  $\Delta V_{2opt}$ . Then <sup>4</sup>

$$\Delta V_{Tot Opt} = \Delta V_{1opt} + \Delta V_{2opt} \quad (99).$$

### Restricted Three-Impulse Plane Change

The Restricted Three-Impulse Plane Change<sup>4</sup> rotates a circular orbit by an angle  $\theta$ . For this transfer the radii of the initial and final orbits are equal. Figure 15 represents this maneuver. The first impulse places the spacecraft onto a semi-ellipse at perigee. At

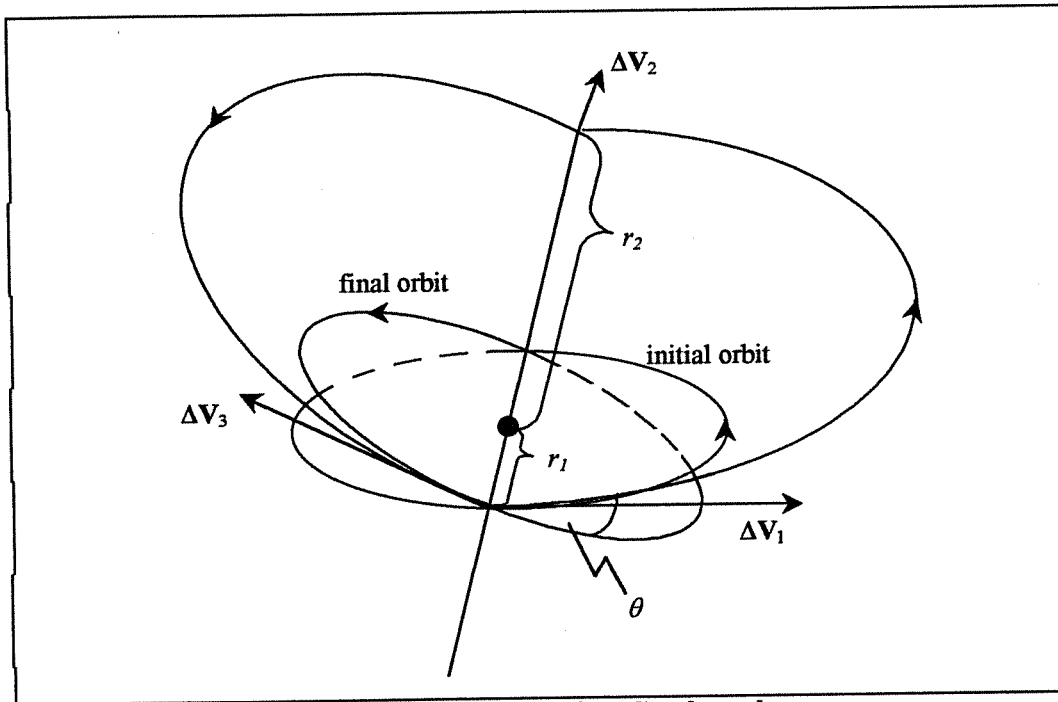


Figure 15 Restricted three-impulse plane change

apogee of this ellipse, a second impulse changes the inclination by  $\theta$ . The spacecraft returns on a similar semi-ellipse to the location of the first impulse. At this point, a third impulse, equal in magnitude to the first, places the spacecraft onto the final circular orbit.

Now,

$$\Delta V_{Tot} = \Delta V_1 + \Delta V_2 + \Delta V_3 \quad (100),$$

$$\frac{\Delta V_1}{V_{c1}} = \frac{\Delta V_3}{V_{c1}} = \sqrt{\frac{2(r_2/r_1)}{1+(r_2/r_1)}} - 1 \quad (101),$$

$$\frac{\Delta V_2}{V_{c1}} = 2\sqrt{\frac{2}{(r_2/r_1)[1+(r_2/r_1)]}} \sin \frac{\theta}{2} \quad (102).$$

$$\frac{\partial \left( \frac{\Delta V_{Tot}}{V_{c1}} \right)}{\partial (r_2/r_1)} = 2 \left[ \begin{aligned} & \sqrt{\frac{2(r_2/r_1)}{[1+(r_2/r_1)]}} \left( -\frac{\sin \frac{\theta}{2}}{(r_2/r_1)^2} \right) \\ & + \left( 1 + \frac{\sin \frac{\theta}{2}}{(r_2/r_1)} \right) \left( \frac{1}{2\sqrt{2(r_2/r_1)/(1+(r_2/r_1))}} \left[ \frac{(1+(r_2/r_1))2 - 2(r_2/r_1)}{(1+(r_2/r_1))^2} \right] \right) \end{aligned} \right] = 0 \quad (104)$$

Solving equation 103 for  $r_2/r_1$  finds the optimal  $(r_2/r_1)_{opt}$  as

$$(r_2/r_1)_{opt} = \frac{\sin \frac{\theta}{2}}{1 - 2 \sin \frac{\theta}{2}} \quad (105).$$

Examining this equation shows that for  $0 \leq \theta \leq 38.94^\circ$ ,  $r_2/r_1 = 1$  should be used. For  $38.94^\circ \leq \theta \leq 60^\circ$ , equation 104 should be used. For  $60^\circ \leq \theta \leq 180^\circ$ ,  $r_2/r_1 = \infty$  should be used.

Similar to the Restricted Three-Impulse Plane Change maneuver is the General Three-Impulse Plane Change maneuver. In the general case, inclination changes are applied at all three impulses, with the first and third angles being equal<sup>4</sup>. Both of these maneuvers can be combined with the bi-elliptic transfer method. In this way plane changes can be combined with change in orbit size.

Using a three-impulse method over a two-impulse method to perform a plane change has one major advantage. The plane change, or largest plane change, can be performed at the apogee of the transfer ellipse. At this point the spacecraft is farthest from the attracting body and has a minimum velocity. Thus a smaller increment is needed to obtain the desired rotation.

The question remains though, how many impulses are necessary? Edelbaum addressed this question<sup>5</sup>. He determined that generally, a transfer in three dimensions requires six impulses. A transfer in two dimensions requires only four. When the position of the spacecraft on the final orbit does not matter, these numbers are five and three respectively.

## **Finite Burns**

Impulsive maneuvers assume the ability to provide an infinite amount of thrust instantaneously. In reality, a finite amount of thrust is provided over some period of time. Methods to optimize finite thrust maneuvers are generally of two types, direct or indirect. Indirect methods use calculus of variations to derive conditions for optimality. This type of method produces a two-point boundary value. Direct methods approximate continuous problem with a parameter optimization problem. Both types of methods are usually solved with mathematical programming and an initially guessed solution. Both types of methods are presented here.

### **Indirect**

This type of method originates from the work of Lawden and his primer vector. Similar to Lawden's work, the trajectory is assumed to be comprised of maximum thrust arcs connected by null thrust arcs. The following method assumes that the trajectory is made up of  $e$  phases. These are separated by internal boundaries and are contained within the external boundaries of the terminal orbits<sup>6</sup>.

During the  $j^{\text{th}}$  phase, the initial radius, circular velocity, and initial spacecraft mass are given as

$$\frac{d\mathbf{r}}{dt} = \mathbf{V} \quad (106),$$

$$\frac{d\mathbf{V}}{dt} = \frac{\mathbf{T}_j}{m} - \frac{\mathbf{r}}{r^3} \quad (107),$$

$$\frac{dm}{dt} = -q_j \quad (108).$$

Here  $T_j$  and  $q_j$  are constants. Obviously,  $q_j = 0$  during null thrust or coast arcs. Equations 105 – 107, must be integrated from time  $t_{j-1}$  to  $t_j$ . Now, if

$$dt = (t_j - t_{j-1})d\varepsilon = \tau_j d\varepsilon \quad (109),$$

then  $\varepsilon$  is a time-like variable which increases by one after each phase. This now becomes a fixed time problem with<sup>6</sup>

$$\dot{\mathbf{r}} = \tau_j \mathbf{V} \quad (110),$$

$$\dot{\mathbf{V}} = \tau_j \left( \frac{\mathbf{T}_j}{m} - \frac{\mathbf{r}}{r^3} \right) \quad (111),$$

$$\dot{m} = -\tau_j q_j \quad (112),$$

$$\dot{t} = 0 \quad (113),$$

which must be integrated from  $\varepsilon = 0$  to  $\varepsilon = e$ . In equations 109-112, (·) denotes differentiation with respect to  $\varepsilon$ .

According to optimal control theory, the Hamiltonian is

$$H = \tau_j \left[ \lambda_r \mathbf{V} + \lambda_v \left( \frac{\mathbf{T}_j}{m} - \frac{\mathbf{r}}{r^3} \right) - \lambda_m q_j \right] = \tau_j H_j^* \quad (114)$$

and the co-state vectors are defined by

$$\dot{\lambda}_r = -\frac{\partial H}{\partial \mathbf{r}} = -\tau_j \frac{\partial H_j^*}{\partial \mathbf{r}} \quad (115),$$

$$\dot{\lambda}_v = -\frac{\partial H}{\partial \mathbf{V}} = -\tau_j \frac{\partial H_j^*}{\partial \mathbf{V}} \quad (116),$$

$$\dot{\lambda}_m = -\frac{\partial H}{\partial m} = -\tau_j \frac{\partial H_j^*}{\partial m} \quad (117).$$

$\lambda_v$ , the co-state vector to the velocity, is what Lawden referred to as the primer vector. Equations 109-112 and 114-116 come with an equal number of external boundary conditions. These derive from the constraints for the states and the transversality conditions for the co-states<sup>6</sup>.

The  $e$  conditions, imposed at the beginning of each phase,

$$\frac{\partial H}{\partial \tau_j} = H_j^* = 0 \quad (118)$$

determine the optimal phase lengths. The Hamiltonian vanishes along the entire trajectory, the state and co-state variables are continuous. At the internal boundaries, equation 117 becomes

$$\lambda_v \frac{\mathbf{T}_j}{m} - \lambda_m q_j = 0 \quad (119).$$

By a similar differentiation of the Hamiltonian the optimal thrust direction control,  $\mathbf{T}_j/T_j$ , can be obtained<sup>6</sup>.

Now, a classical boundary value problem is formed with non-linear constraints at both internal and external boundaries. The problem now consists of  $e$  systems of  $n$  differential equations

$$\dot{\mathbf{x}} = \mathbf{f}_j(\mathbf{x}, \mathbf{u}(\mathbf{x})) \quad (120)$$

to be integrated from  $\varepsilon = 0$  to  $\varepsilon = e$  with the  $n$  boundary conditions

$$\mathbf{h}(\mathbf{x}(0), \mathbf{x}(1), \dots, \mathbf{x}(j), \dots, \mathbf{x}(e)) = 0 \quad (121).$$

The solution is obtained by reducing the boundary value problem to a series of initial value problems brought to convergence by Newton's method.

## Direct

The Direct method presented here converts the optimal control problem to a nonlinear programming problem using collocation with Hermite cubics. It is referred to as direct collocation with nonlinear programming (DCNLP)<sup>7</sup>.

The trajectory is approximated by piecewise polynomials represented by state and control values at several nodes. For a given state variable, the state trajectory between two nodes is the cubic that has the derivatives at the endpoint that are determined by the evaluation of the differential equations of motion at the endpoints. At a point in the center of this segment, the derivative of this cubic is compared to the derivative from the equations of motion<sup>7</sup>. This point is referred to as a collocation point and the difference found is called the defect. This defect is a sign of how well the equations of motion are satisfied over the segment.

Given a state vector  $\mathbf{x}$ , control vector  $\mathbf{u}$ , and the length in time over a segment as  $T$ , if the equations of motion are given by<sup>8</sup>

$$\dot{\mathbf{x}} = f(\mathbf{x}, \mathbf{u}) \quad (122),$$

then state vector interpolated at the collocation point is

$$\mathbf{x}_c = (1/2)(\mathbf{x}_l + \mathbf{x}_r) + (T/8)[f(\mathbf{x}_l) - f(\mathbf{x}_r)] \quad (123),$$

where  $\mathbf{x}_l$  and  $\mathbf{x}_r$  are the state vectors at the left and right nodes respectively. The control vector is linearly interpolated as

$$\mathbf{u}_c = (1/2)(\mathbf{u}_l + \mathbf{u}_r) \quad (124).$$

The derivative of the interpolating cubic at the collocation point is

$$\dot{\mathbf{x}}_c = -\frac{3}{2T}(\mathbf{x}_l - \mathbf{x}_r) - \frac{1}{4}[f(\mathbf{x}_l) - f(\mathbf{x}_r)] \quad (125)$$

and the defect vector is

$$\mathbf{d} = f(\mathbf{x}_c, \mathbf{u}_c) - \dot{\mathbf{x}}_c \quad (126).$$

When  $\mathbf{x}_l, \mathbf{u}_l, \mathbf{x}_r, \mathbf{u}_r$  are chosen to minimize  $d$ , the polynomials provide an accurate approximation to the equations of motion.

Now the problem can be converted to a nonlinear programming problem. The objective function, defects and problem constraints can be calculated from the state and control vectors at the nodes.

A finite thrust trajectory can be described by figure 17 and the following equations of motion

$$\left. \begin{aligned} \dot{x}_1 &= x_3 \\ \dot{x}_2 &= \frac{x_4}{x_1} \\ \dot{x}_3 &= \frac{x_4^2}{x_1} - \frac{1}{x_1^2} + x_5 \sin u_1 \\ \dot{x}_4 &= -\frac{x_3 x_4}{x_1} + x_5 \cos u_1 \\ \dot{x}_5 &= \frac{x_5^2}{c} \end{aligned} \right\} (127).$$

In these equations,  $x_1$  is the radius,  $x_2$  is the angle from a reference direction,  $x_3$  is the radial velocity,  $x_4$  is the tangential velocity,  $x_5$  is the thrust acceleration,  $u_1$  is the thrust vector angle, and  $c$  is the exhaust velocity.

The trajectory is divided into segments of constant and null thrust arcs. The constant thrust arcs are further divided into even segments. For each of these segments collocation defects are calculated from the states and controls at the segment nodes and the length of the thrust arc. The null arc has an analytical solution. Integrals of the motion are calculated using the state vectors at each end. The defect for the null thrust

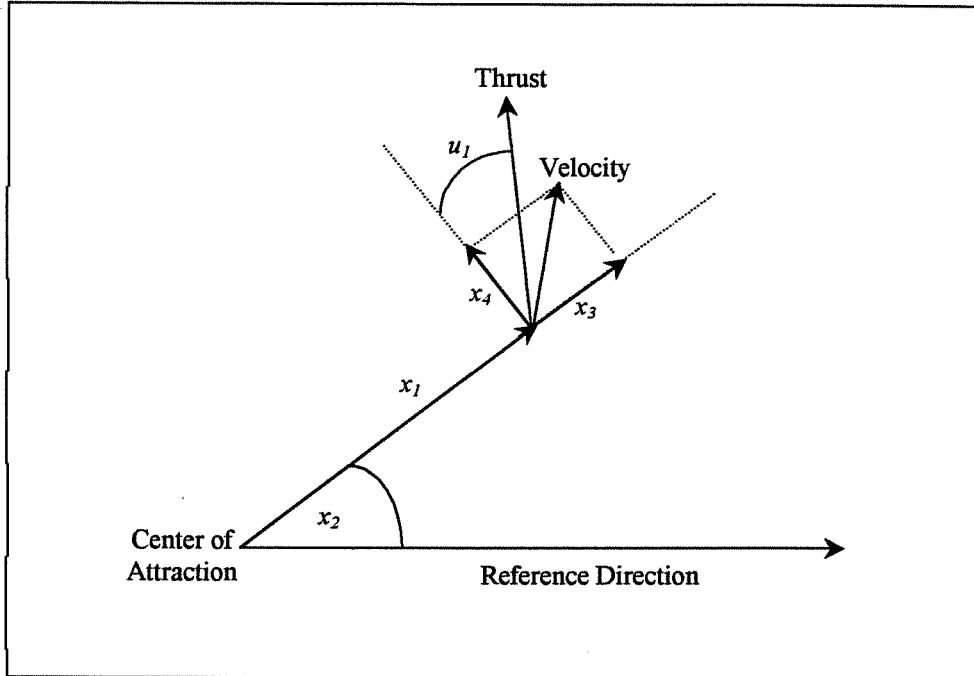


Figure 17 State and control variables

arc is calculated as the difference between the integrals at the two nodes, or

$$q_i = Q_i(x_l) - Q_i(x_r) \quad (128).$$

Here  $q_i$  is the  $i$ th generalized defect for the given arc,  $Q_i$  is the  $i$ th integral of the motion, and  $x_l$  and  $x_r$  are the state vectors for the left and right nodes respectively<sup>7</sup>.

For the two-dimensional thrust free orbit equations (equations 126 with  $x_5 = 0$ ), there are three constants of the motion<sup>7</sup>. Angular momentum, energy, and longitude of periapsis are usually chosen. Since no mass is expelled during a null thrust arc, the thrust acceleration is the same at both ends of the arc. This provides the fourth integral. These integrals are

$$\left. \begin{aligned}
 Q_1(x) &= x_1 x_4 \\
 Q_2(x) &= \frac{x_3^2 + x_4^2}{2} - \frac{1}{x_1} \\
 Q_3(x) &= x_2 + \tan^{-1} \left[ \frac{-x_3 x_4}{x_4^2 - \frac{1}{x_1}} \right] \\
 Q_4(x) &= x_5
 \end{aligned} \right\} (129).$$

Typically, nonlinear programming routines need the derivatives of the objective function and the constraints with respect to the variables. For the collocation defects, this means chain-rule differentiation of equations 122-126. As an example, the defect vector differentiated with respect to the state vector at the left end of the segment would be given by<sup>7</sup>

$$\mathbf{F}(\mathbf{x}_c, \mathbf{u}_c) \left[ \frac{\mathbf{I}_5}{2} + \frac{T}{8} \mathbf{F}(\mathbf{x}_l, \mathbf{u}_l) \right] + \frac{3}{2T} \mathbf{I}_5 + \frac{\mathbf{F}(\mathbf{x}_l, \mathbf{u}_l)}{4} \quad (130).$$

$\mathbf{I}_5$  is the 5x5 identity matrix and  $\mathbf{F}(\mathbf{x}, \mathbf{u})$  is the 5x5 matrix produced by differentiation of the right side of the equations of motion  $f(\mathbf{x}, \mathbf{u})$  with respect to the state vector  $\mathbf{x}$ . Similar calculations are done for the derivatives of the defect with respect to the right state vector, the left and right control vectors, and the thrust arc duration. Differentiating equations 128 with respect to the state vector provides the derivatives of the generalized defects. Usually, the objective function is the sum of the thrust arc durations, so its derivative does not matter. Any other problem constraints must also be differentiated.

For the nonlinear programming (NLP) problem, the state and control vectors at the nodes and the thrust arc durations are collected into the NLP state vector  $\mathbf{X}$ :

$$\mathbf{X}^T = [\mathbf{x}_1^T, \mathbf{u}_1^T, \mathbf{x}_2^T, \mathbf{u}_2^T, \dots, \mathbf{x}_n^T, \mathbf{u}_n^T, t_1, t_2, \dots, t_k] \quad (131).$$

Here  $n$  is the total number of nodes and  $k$  is the number of thrust arcs. Defects, generalized defects and other constraints are collected into the NLP constraint vector  $\mathbf{C}$ :

$$\mathbf{C}^T = [\mathbf{g}_1^T, \mathbf{g}_2^T, \dots, \mathbf{g}_{n-1}^T, \mathbf{w}^T] \quad (132).$$

Here  $\mathbf{g}_i$  is either the defect vector of the corresponding thrust arc or the vector of generalized defects for the corresponding null thrust arc.  $\mathbf{w}$  is a vector of any additional constraints.

The NLP problem is solved using a Lagrangian method that solves a sequence of quadratic programming problems that approximate the nonlinear problem. Enright and Conway used this method to solve two and three burn circle to circle transfers with canonical units<sup>7</sup>. Figure 18 shows the two-burn problem. This is similar to the Hohmann transfer with finite instead of impulsive thrust. The trajectory was divided into two thrust arcs separated by a null thrust arc. The thrust arcs were then divided into 12 segments each. Figure 19 represents the three-burn problem. This trajectory was divided into three thrust arcs separated by two null thrust arcs. The first two thrust arcs occur near periapsis with one orbital revolution between them. All three thrust arcs were divided into 10 segments.

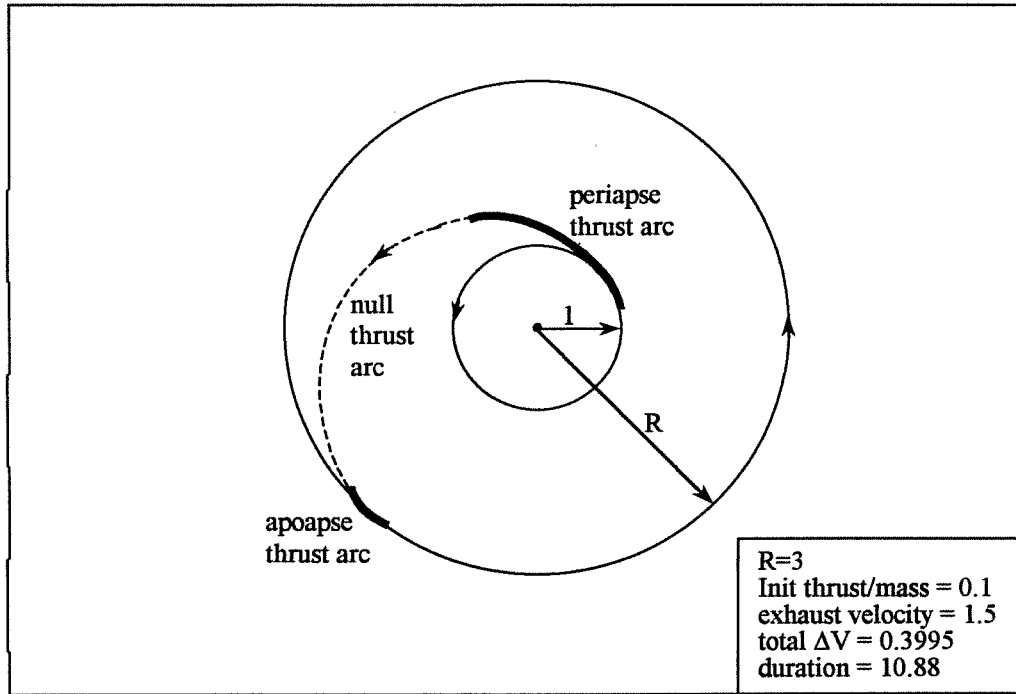


Figure 18 Two-burn finite thrust transfer trajectory

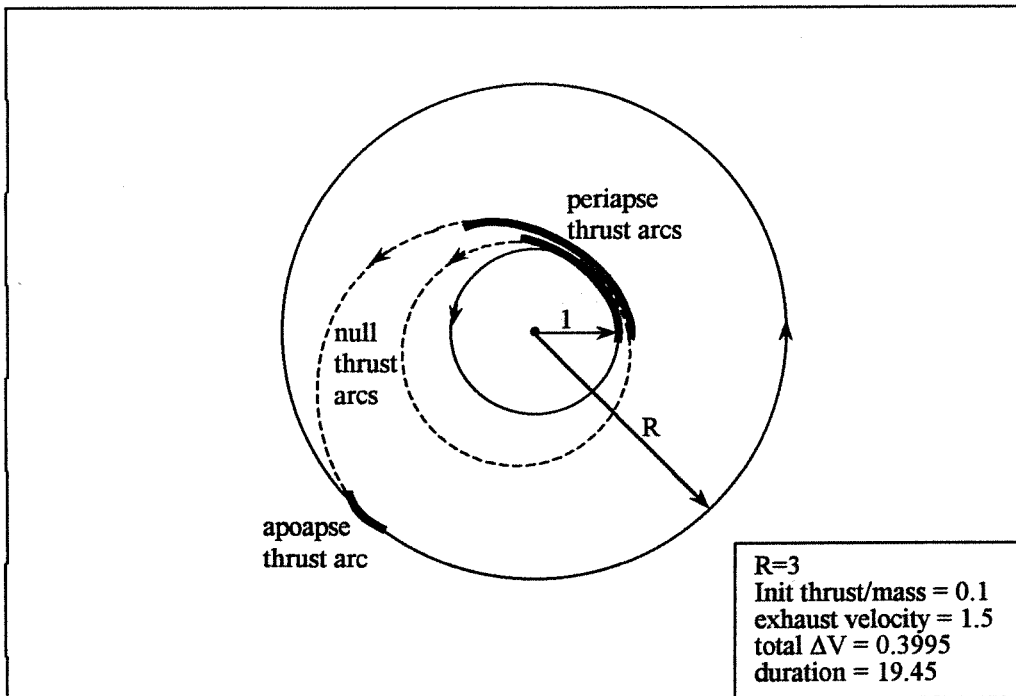


Figure 19 Three-burn finite thrust transfer trajectory

## Low Thrust

In most low thrust transfer cases the thrust is applied continuously throughout the maneuver. For this reason, minimum fuel usage usually occurs with minimum transfer time and the problem becomes one of optimal steering. In 1961, Edelbaum studied the use of low thrust to perform small changes in orbital elements.

Edelbaum represented the thrust force in three components<sup>9</sup>, one tangent to the velocity,  $F_T$ , one normal to the orbit plane,  $F_N$ , and one normal to the previous two,  $F_Z$ .

These three components can be given by

$$\begin{aligned} F_T &= F \cos \beta \cos \alpha \\ F_N &= F \cos \beta \sin \alpha \\ F_Z &= F \sin \beta \end{aligned} \quad (133)$$

where  $\alpha$  is the angle between the velocity vector and the component of the thrust vector in the plane of the orbit, and  $\beta$  is the angle between the thrust vector and the plane of the orbit. For orbits with small eccentricity and inclination, the equations of motion are

$$\begin{aligned} \frac{di}{dt} &= \frac{\cos(\omega + \theta) F_Z}{V_0 m} \\ \frac{d\Omega}{dt} &= \frac{\sin(\omega + \theta) F_Z}{iV_0 m} \\ \frac{da}{dt} &= \frac{2a F_T}{V_0 m} \\ \frac{de}{dt} &= \frac{2 \cos \theta F_T}{V_0 m} + \frac{\sin \theta F_N}{V_0 m} \\ \frac{d\omega}{dt} &= \frac{2 \sin \theta F_T}{eV_0 m} + \frac{\cos \theta F_N}{eV_0 m} - \frac{\sin(\omega + \theta) F_Z}{iV_0 m} \end{aligned} \quad (134)$$

where  $i$  is inclination,  $\omega$  is argument of perigee,  $\theta$  is the position angle from perigee,  $V_0$  the initial velocity,  $m$  the mass,  $\Omega$  the longitude of the ascending node,  $a$  the semi-major axis, and  $e$  the eccentricity. Combining equations 132 and 133 yields

$$\begin{aligned}\frac{da/a_0}{dt} &= \frac{F}{mV_0}(2 \cos \alpha \cos \beta) \\ \frac{de}{dt} &= \frac{F}{mV_0}(2 \cos \theta \cos \alpha \cos \beta + \sin \theta \sin \alpha \sin \beta) \quad (135). \\ \frac{di}{dt} &= \frac{F}{mV_0}[\cos(\omega + \theta) \sin \beta]\end{aligned}$$

The optimal steering can be found by combining these equations with Lagrange multipliers and setting the partial derivatives with respect to the steering angles  $\alpha$  and  $\beta$  to zero<sup>9</sup>

$$\frac{\partial}{\partial \alpha} \frac{\partial}{\partial \beta} \left[ \frac{da/a_0}{dt} + \lambda_1 \frac{de}{dt} + \lambda_2 \frac{di}{dt} \right] = 0 \quad (136).$$

Substituting equation 134 into 135 can produce solutions for the optimal steering angles  $\alpha_{opt}$  and  $\beta_{opt}$

$$\begin{aligned}\tan \alpha_{opt} &= \frac{\lambda_1 \sin \theta}{2(1 + \lambda_1 \cos \theta)} \\ \tan \beta_{opt} &= \frac{\lambda_2 \cos(\omega + \theta)}{\sqrt{4(1 + \lambda_1 \cos \theta)^2 + \lambda_1^2 \sin^2 \theta}}\end{aligned} \quad (137).$$

As a special case, Edelbaum derived the case of large changes in inclination between the initial and final orbits. This case assumes that the orbit remains quasi-circular and that the thrust direction is a constant. This second assumption makes the change in inclination<sup>9</sup>

$$di = \frac{2}{\pi} \frac{F \sin \beta}{mV} dt \quad (138).$$

The velocity will decrease as the major axis increases

$$dV = -\frac{F}{m} \cos \beta dt \quad (139).$$

The variational integrand to be optimized is

$$-\int \left( \frac{di}{dV} + \lambda \frac{dt}{dV} \right) dV = \int \left( \frac{2 \tan \beta}{\pi V} + \frac{\lambda m}{F \cos \beta} \right) dV \quad (140).$$

The partial derivative with respect to the thrust angle should be zero

$$\frac{\partial}{\partial \beta} \left( \frac{2 \tan \beta}{\pi V} + \frac{\lambda m}{F \cos \beta} \right) = 0 \quad (141)$$

which reduces to

$$V \sin \beta = \frac{2F}{m\pi\lambda} = \text{const} = V_0 \sin \beta_0 \quad (142).$$

Now, equations 137 and 138 can be integrated

$$\left. \begin{aligned} \frac{F}{m} dt &= -\frac{dV}{\cos \beta} - \frac{dV}{\sqrt{1 - \sin^2 \beta \frac{V_0^2}{V^2}}} \\ \frac{F}{m} dt &= -\frac{dV}{2\sqrt{V^2 - V_0^2 \sin^2 \beta_0}} \\ ft = \Delta V &= V_0 \cos \beta_0 - \sqrt{V^2 - V_0^2 \sin^2 \beta_0} \\ V &= \sqrt{V_0^2 - 2V_0 \Delta V \cos \beta_0 + \Delta V^2} \end{aligned} \right\} \quad (143)$$

$$\left. \begin{aligned} di &= -\frac{2 \tan \beta}{\pi V} dV \\ di &= -\frac{2 V_0 \sin \beta dV}{\pi V \sqrt{V^2 - V_0^2 \sin^2 \beta_0}} \\ i &= \frac{2}{\pi} \sin^{-1} \frac{V_0 \sin \beta_0}{V} - \frac{2\beta_0}{\pi} \end{aligned} \right\} \quad (144).$$

Equations 142 and 143 can combine to form

$$\left. \begin{aligned}
a) \frac{\Delta V}{V_0} &\leq \cos \beta_0 \\
i &= \frac{2}{\pi} \sin^{-1} \frac{V_0 \sin \beta_0}{\sqrt{V_0^2 - 2V_0 \Delta V \cos \beta_0 + \Delta V^2}} - \frac{2\beta_0}{\pi} \\
b) \frac{\Delta V}{V_0} &\geq \cos \beta_0 \\
i &= 114.6^\circ - \frac{2}{\pi} \sin^{-1} \frac{V_0 \sin \beta_0}{\sqrt{V_0^2 - 2V_0 \Delta V \cos \beta_0 + \Delta V^2}} - \frac{2\beta_0}{\pi}
\end{aligned} \right\} (145).$$

Equations 142 and 144 represent the change in velocity and inclination as the initial steering angle is changed. When solved simultaneously, these equations can find the characteristic velocity requirements in terms of velocity and inclination

$$\Delta V = \sqrt{V_0^2 - 2V_0 \cos \frac{\pi}{2} i + V^2} \quad (146).$$

In 1992, Kechichian reformulated Edelbaum's work using optimal control theory<sup>10</sup>. With knowledge of the elements of the initial and final orbits and knowing that

$$\begin{aligned}
V_0 &= \left( \frac{\mu}{a_0} \right)^{1/2} \\
V_f &= \left( \frac{\mu}{a_f} \right)^{1/2}
\end{aligned} \quad (147),$$

the initial steering angle  $\beta_0$  can be calculated using

$$\tan \beta_0 = \frac{\sin \frac{\pi}{2} \Delta i}{\frac{V_0}{V_f} - \cos \frac{\pi}{2} \Delta i} \quad (148).$$

The total  $\Delta V$  of this maneuver can be found from

$$\Delta V = V_0 \cos \beta_0 - \frac{V_0 \sin \beta_0}{\tan \left( \frac{\pi}{2} \Delta i + \beta_0 \right)} \quad (149).$$

Since  $\Delta V = Ft$ , the total transfer time can be calculated from  $t_f = \Delta V_{Tot}/F$ . The variation with time of the variables of interest in this maneuver are given by

$$\begin{aligned}\beta &= \tan^{-1}\left(\frac{V_0 \sin \beta_0}{V_0 \cos \beta_0 - Ft}\right) \\ V &= (V_0^2 - 2V_0 Ft \cos \beta_0 + F^2 t^2)^{1/2} \\ \lambda_v &= \frac{\cos \beta}{F} \\ \Delta i &= \frac{2}{\pi} \left[ \tan^{-1}\left(\frac{Ft - V_0 \cos \beta_0}{V_0 \sin \beta_0}\right) + \frac{\pi}{2} - \beta_0 \right]\end{aligned}\quad (150).$$

As an example, consider the transfer from an initial orbit with  $a_0 = 7000$  km and  $i_0 = 28.5^\circ$  to a final orbit with  $a_f = 42166$  km and  $i_f = 0^\circ$ . With a thrust acceleration of  $F = 3.5 \times 10^{-7}$ , the maneuver takes 191 days,  $\Delta V_{Tot} = 5.78$  km/s, and the steering angle  $\beta$  varies from  $\beta_0 = 21.98^\circ$  to  $\beta_f = 66.61^\circ$ . Figures 20 through 22 show the variation of  $\beta$ ,  $V$ , and  $i$  with time respectively<sup>10</sup>.

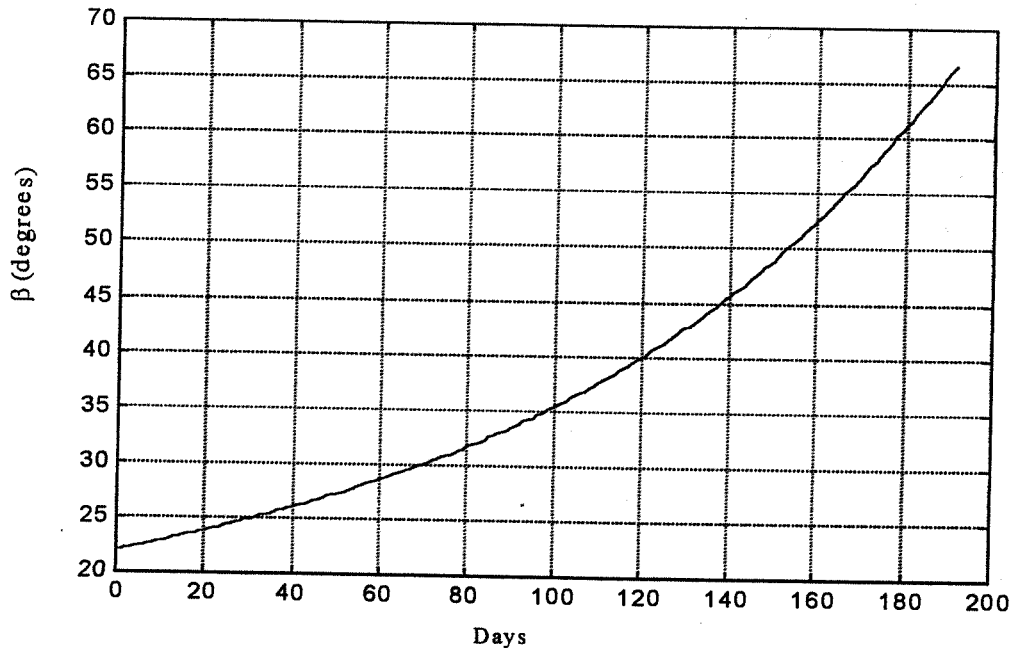
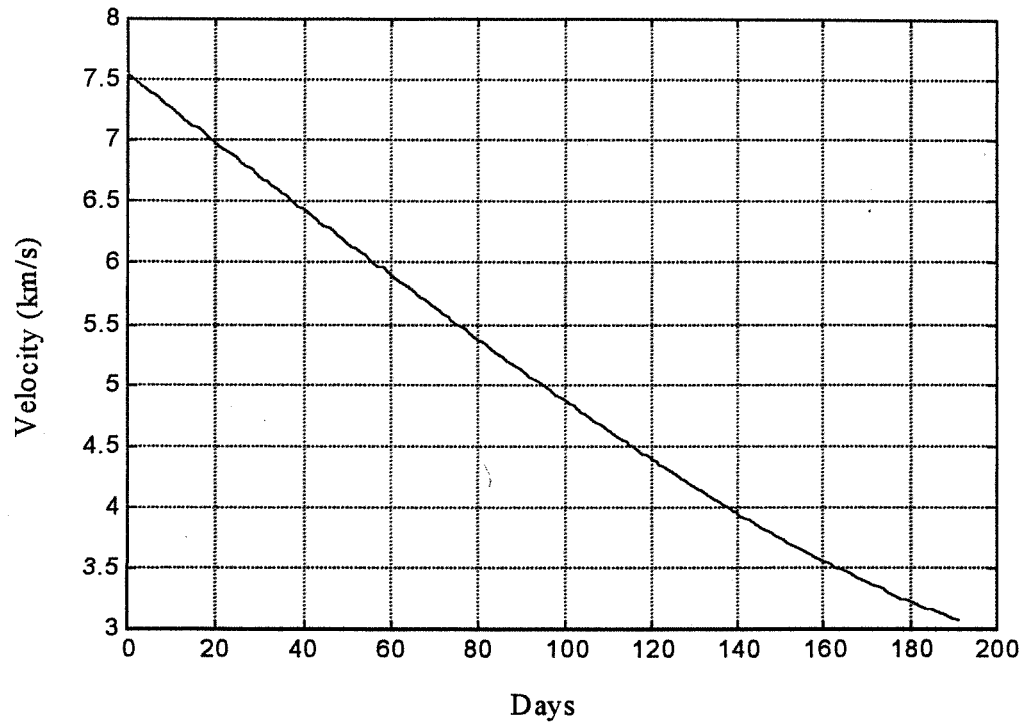
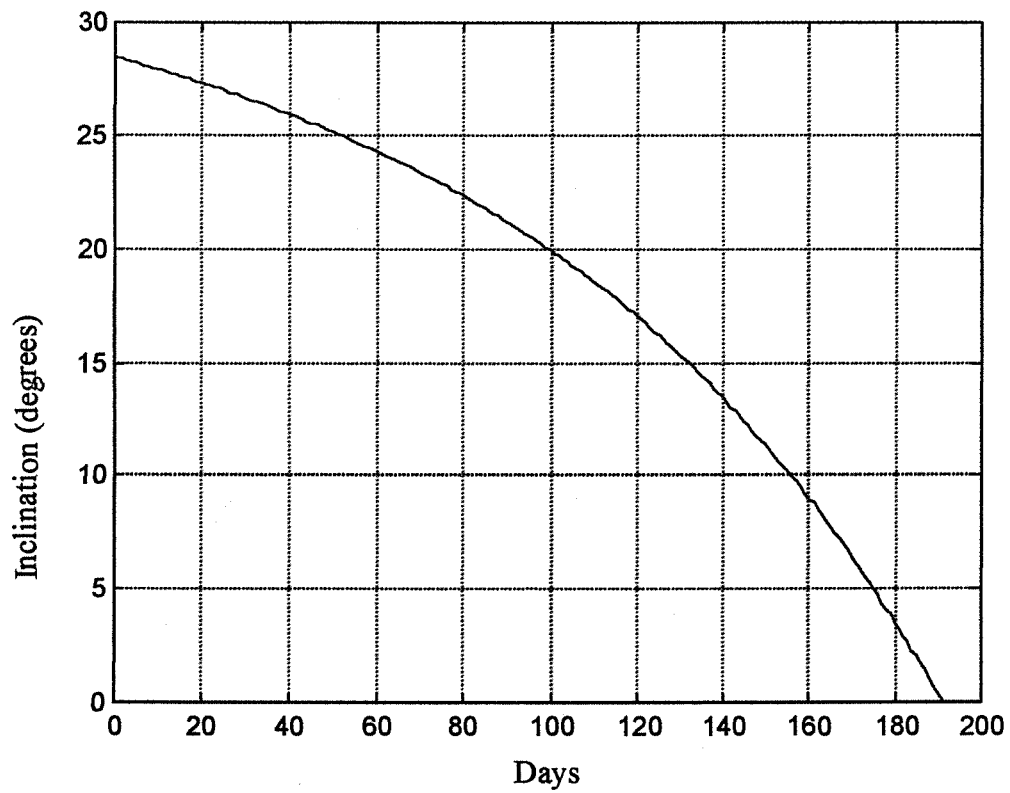


Figure 20 Steering angle versus time



**Figure 21 Velocity versus time**



**Figure 22 Inclination versus time**

## Conclusion

Methods have been presented to transfer between orbits in a manner to minimize  $\Delta V$ . The choice of which method to employ would depend on the propulsion system chosen. Impulsive transfers require the ability to provide large amounts of thrust in short bursts, but require less time to complete. Low thrust transfers may need a much longer time frame for completion. Low thrust electric propulsion systems are very efficient, but require large power systems, which add to launch weight and therefore cost.

The methods here aim to optimize propellant use. Sometimes there may be other optimization requirements. Certain missions, especially those with human passengers, need to minimize transfer time. Most times there will be a tradeoff between the two.

## References

1. Lawden, D. F., *Optimal trajectories for Space Navigation*, Butterworths & Co., Ltd, London, 1963
2. Lawden, D. F., "Impulsive Transfer Between Elliptical Orbits," *Optimization Techniques*, edited by G. Leitmann, Academic Press, New York, 1962, Chap. 11
3. Hoelker, R.F. and Silber R., "The Bi-Elliptical Transfer Between Coplanar Circular Orbits." *Proceedings of the Fourth AFBMD/STL Symposium-Advances in Ballistic Missile and Space Technology Vol. 3*, Pergamon Press, New York, 1961
4. Chobotov, V. ed., "Orbital Maneuvers," *Orbital Mechanics*, AIAA Education Series, Washington D.C., 1991
5. Edelbaum, T.N., "How Many Impulses" *Aeronautics and Astronautics*, Nov 1967
6. Colasurdo, G., "Optimal Finite-Thrust Spacecraft Trajectories", AIAA-92-4510-CP *AIAA/AAS Astrodynamics Conference*, Hilton Head Island, SC August 10-12, 1992
7. Enright, P.J. and Conway, B.A., "Optimal Finite-Thrust Spacecraft Trajectories Using Collocation and Nonlinear Programming," *Journal of Guidance, Control and Dynamics*, Vol. 14, No. 5 1991
8. Hargraves, C.R. and Paris, S.W., "Direct Trajectory Optimization Using Nonlinear Programming and Collocation," *Journal of Guidance, Control, and Dynamics*, Vol. 10, No. 4, 1987
9. Edelbaum, T.N., "Propulsion requirements for Controllable Satellites," *ARS Journal*, Aug 1961
10. Kechichian, J.A., "The Reformulation of Edelbaum's Low-Thrust Transfer Problem Using Optimal Control Theory", AIAA-92-4576-CP *AIAA/AAS Astrodynamics Conference*, Hilton Head Island, SC August 10-12, 1992
11. Larson, W.J. and Wertz, J.R., eds, *Space Mission Analysis and Design*, Microcosm, Inc, California, 1992